Chem Soc Rev

Chemical Sensing of Neurotransmitters

Journal:	*Chemical Society Reviews*
Manuscript ID:	CS-REV-12-2013-060477.R1
Article Type:	Review Article
Date Submitted by the Author:	28-Mar-2014
Complete List of Authors:	Pradhan, Tuhin; Korea University, Department of chemistry Jung, Hyo Sung; Korea University, Chemistry Jang, Joo Hee; Korea University, Chemistry Kim, Tae Woo; Graduate School of East-West Medicine, Kang, Chulhun ; Kyunghee University , The school of east-west medical science Kim, Jong Seung; Korea University, Chemistry

Chemical Sensing of Neurotransmitters

Tuhin Pradhan,[a,c] Hyo Sung Jung,[a] Joo Hee Jang,[a] Tae Woo Kim,[b] Chulhun Kang*[b] and Jong Seung Kim*[a]

Receipt/Acceptance Data **[DO NOT ALTER/DELETE THIS TEXT]**
Publication data **[DO NOT ALTER/DELETE THIS TEXT]**
DOI: 10.1039/b000000x [DO NOT ALTER/DELETE THIS TEXT]

In the past decades, the development of chemosensors for neurotransmitter has recently emerged as a research area of significant importance, which attracted a tremendous amount of attention to its high sensitivity and rapid response. This current review focuses on various neurotransmitter detection based on fluorescent or colorimetric spectrophotometry published for the last 12 years, covering biogenic amines (dopamine, epinephrine, norepinephrine, serotonin, histamine and acetylcholine), amino acids (glutamate, aspartate, GABA, glycine and tyrosine), and adenosine.

Introduction

Neurotransmitters are endogenous molecules transmitting an electrical impulse from a nerve cell to another nerve, muscle, organ, or other tissues to play roles as messengers of neurologic information. Upon electrical stimulations on a neuron, the neurotransmitters stored within the synaptic vesicles in its synapses are released into the synaptic cleft *via* exocytosis to activate post-synaptic receptors and initiate the next round of signalling pathways.[1] A number of factors such as poor diet, toxic chemicals, infections, stress, and genetic factors may disrupt this neurologic signal transmission through imbalancing the neurotransmitter levels to cause many clinical conditions including psychiatric disorders.[2]

Since a neurotransmitter, identified as acetylcholine later, had been described by Otto Loewi at 1921,[3] upto now, about 100 neurotransmitters have been known. According to the chemical structures, they can be grouped into several classes such as biogenic amines (e.g., dopamine, epinephrine, norepinephrine, serotonin, histamine and acetylcholine), amino acids (primarily glutamic acid, aspartic acid, γ-aminobutyric acid [GABA], and glycine), peptides (e.g., vasopressin, somatostatin, neurotensin, and enkephalines), and gaseous neurotransmitters (nitric oxide, carbon monoxide, and hydrogen sulfide).

Many different approaches have been attempted for the reliable determination of neurotransmitters *in vivo* and *in vitro*. Widely-adopted analytical strategy is 'separation and detection' such as liquid chromatography (LC), capillary electrophoresis (CE), capillary electro-chromatography coupled with UV detection, flow immunoassay, native fluorescence detection, and electrochemical detection. However, there are increasing demands for new experimental methods since elucidation of the neurotransmitter metabolisms and their functions, the critical information in understanding neuroscience, requires further improvement of the analysis tools in this field to overcome the limitations of the current methods.[4] For instance, the chromatographic method has a long operation time and the limited spatial resolution. And, selectivity of the electrochemical neurotransmitter sensors may be hampered by the presence of other molecules with the similar redox potentials to that of the target molecule although they can provide millisecond-range responses with micrometer-range resolution.

For detection of neurotransmitter, the fluorescence-based optical methods may be valuable to overcome other techniques' weak points since they have fast response time and simple procedures and non-destructive,[5-16] which allow the applications to a variety of physiological samples. Therefore, a sensitive analytical method based on a fluorescence probe designed to detect a neurotransmitter selectively will provide fast, reliable and more substantial information on the localization and quantity of the target molecule of interest. Indeed, several fluorescence-based sensing devices have been reported for various neurotransmitters.

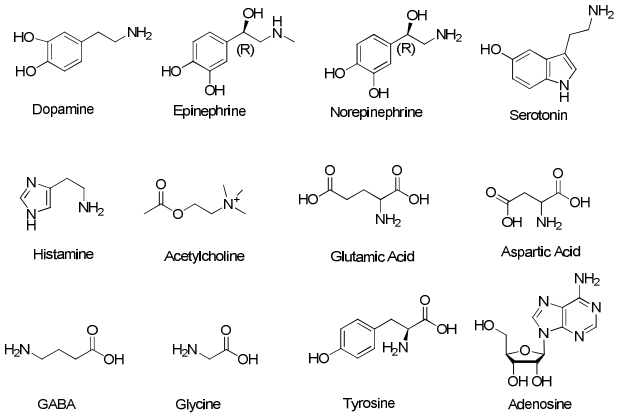

Fig. 1 Chemical structures of some neurotransmitters.

In this current review, we sought to reveal the substantial progresses in neurotransmitter-sensing for the last 12 years, covering biogenic amines (dopamine, epinephrine, norepinephrine, serotonin, histamine and acetylcholine), amino acids (glutamate, aspartate, GABA, glycine and tyrosine), and

[a]*Department of Chemistry, Korea University, Seoul 130-701, Korea; Fax: +82-2-3290-3121; Tel: +82-2-3290-3143; E-mail: jongskim@korea.ac.kr*
[b]*The East-West Medical Science, Kyung Hee University, Yongin 446-701, Korea; E-mail: kangch@khu.ac.kr*
[c]*Vel Tech Rangarajan Dr. Sagunthala R&D Institute of Science and Technology, and Department of Chemistry, Vel Tech Dr. RR & Dr. SR Technical University, Avadi, Chennai-600062, India*

adenosine (the chemical structures of these neurotransmitters are shown in Fig. 1). The chemical sensing of peptide and gaseous neurotransmitters (carbon monoxide, nitric oxide, and hydrogen sulfide) are not summarized in the present article because of lack of the publications and several recent reviews,[6,17-28] respectively.

Some General Design Principles and Photophysical Mechanisms for Chemical Sensing of Neurotransmitters

Fluorescence Resonance Energy Transfer (FRET)

Nonradiative energy transfer occurs between donor and acceptor chromophore molecules through dipole-dipole interactions in FRET process. Two chromophores should be placed in close proximity (<10 nm).[29] Generally, external light source excites the donor fluorophore. Energy transfer efficiencies (κ) depends on the inter-chromophore distance (r) according to the equation, $\kappa = \frac{1}{\tau_D}\left(\frac{R_0}{r}\right)^6$ where τ_D is the donor lifetime in the absence of energy transfer. The parameter, κ is half-maximal when r = R_0 (Forster distance). R_0 depends upon many photophysical parameters, such as quantum yield (φ) of the donor, molar extinction coefficients (ε) of the acceptor, the degree of overlap integral between emission spectrum of donor and excitation spectrum of acceptor and the relative orientation of the fluorophore dipoles in space. FRET has been used as the design principle for the chemical sensors of neurotransmitters. The modulation of FRET process in dyad system can originate the ratiometric measurement in living cells, which reduces the artifacts coming from probe surroundings. This is an advantage of using FRET sensor for the detection of analytes. In presence of analyte, if the cleavage of dyad system occurs, the distance between donor and acceptor becomes infinitive, resulting no energy transfer. Thus, the fluorescence intensity of the donor will increase and that of acceptor will decrease in presence of analyte, which in turn, can be a quantitative measure of analyte concentration.

Photo-induced Electron Transfer (PET)

Photo-induced electron transfer (PET) is the most widely used mechanism for designing of chemical sensors.[30-31] Generally, PET sensor is constructed with three units, fluorophore, receptor and a linking aliphatic spacer. When the electrons of the fluorophore in highest occupied molecular orbital (HOMO) are excited to lowest unoccupied molecular orbital (LUMO), electron transfer occurs from a nearby high lying filled donor orbital (HOMO) resided in receptor to the vacant HOMO (fluorophore), which causes fluorescence quenching. Upon binding of the analyte (neurotransmitter) to the receptor, the energy level of the donor orbital (HOMO) in receptor is lowered, thus slowing down electron transfer to the attached fluorophore (vacant HOMO after excitation), and fluorescence is restored. A major advantage of this mechanism is that it can be used to give an off-to-on signal.

Photo-induced Charge Transfer (PICT)

Photo-induced charge transfer (PICT) is another mechanism for quenching the fluorescence property of a sensor. When a fluorophore molecule has both an electron-pushing (e.g. amino, methoxy) and electron-pulling group conjugated with each other, it undergoes intramolecular charge transfer from the donor to the acceptor upon photo-excitation. PICT can be modulated by varying the strength of the acceptor and donor moiety. Fluorescence quenching takes place when the PICT occurs from the fluorophore moiety to non-fluorophore moiety or vice-versa.[32-35] PICT may cause the increase of dipole moment in excited state and thereby it forms a relaxed ICT state of minimal free energy after complete solvent relaxation. Fluorescence band shift occurs in presence or absence of analyte. This is the origin of ratiometric measurements of analyte concentration at two wavelengths.

Electrostatic Interaction

Electrostatic interaction between host and guest (analyte) induces supramolecular association or host-guest complexation. The electrostatic interaction may be of several kinds, such as ion-dipole or dipole-dipole interactions. If the host molecule possesses fluorescent property, quenching may occur due to this association or complexation and thus analyte concentration can be determined quantitatively from the reduction of fluorescence intensity.

Excimer Formation

Excimer formation has been widely exploited for the design of chemosensors. Excimer is a dimer which is formed at electronic excited state. Pyrene has several photophysical features[36] (e.g. long life time of the excited state) that make it an appropriate fluorophore to form monomer/excimer, probing its microenvironments and thus recognizes several analytes. Generally, excimer exhibits strong and broad band emission spectrum, which is red shifted and well separated with monomer emission band. When one analyte molecule (e.g. neurotransmitter) is attached with two pyrene analogues, pyrene units linked with each other via analyte come in close proximity and induce excimer formation. Analyte concentration in solutions can be estimated from the increase of emission intensity at excimer emission peak wavelength.

Ligand Exchange Method

A ligand exchange method is used somewhere for the development of chemical sensor for the neurotransmitters. Initially, if the 3d-metal ions are complexed with fluorophore analogues, the fluorophore analogues can be displaced with more nucleophilic analytes, which results recovery of the fluorescence emission. The entering groups (i.e., analytes) should have good nucleophilicity and poor (nonlabile) leaving capacity. Usually entering and leaving groups exchange in a single step by forming an activated complex.

Catalytic and Molecular Beacon

Generally, molecular beacons (MBs) are used as fluorescent probes for nucleic acid detection. The conventional molecular

beacon (MB) is built with a stable hairpin (stem-loop) oligonucleotide, of which one end bears a fluorophore and another end bears a quencher unit.[37] When the fluorophore and quencher are no longer in close proximity in the hairpin or closed form, fluorescence is quenched due to efficient fluorescence resonance energy transfer (FRET) between them. The target analyte (e.g. DNA) is a complementary to the loop of the hairpin. In presence of the target analyte (e.g. DNA or neurotransmitter), the MB undergoes a conformational change from closed (hairpin) to open (linear) structure. This process is associated with an increase in fluorescence intensity because of restricting FRET. Hence, the sharp increase in fluorescence intensity determines the presence of the analyte in both qualitative and quantitative manner. The conventional MBs are modified by several research groups for improving specificity towards target analytes and detection limit.

Fluorescence Polarization

Fluorescence polarization or fluorescence anisotropy provides the average angular displacement of the fluorophore that happens during the lifetime of the excited state. The angular displacement depends upon the rate and extent of rotational diffusion during the fluorophore lifetime of the fluorophore, which in turn is dependent upon the size and shape of the rotating fluorophore molecule and viscosity of the solvent. Fluorescence polarization is especially useful for investigating membrane fluidity, protein-DNA interactions etc. This has also been exploited to design the chemical sensors for neurotransmitters. When target analytes are bound with the aptamer (functional olegonucleotides) attached with a fluorophore, structural and conformational changes are occurred in aptamer. These lead to the modified fluorescence polarization signal. The disadvantage of this strategy is that it requires large structural or conformational change in aptamer to get a detectable fluorescence anisotropy response. Sometimes binding of the target analytes with the aptamer causes the displacement of fluorophore-labeled complementary strand from the aptamer unit, resulting reduced fluorescence polarization signal due to the reduction of apparent size of the probe. This approach requires searching of suitable complementary strand that can bind target analyte strongly.[38-39]

Fluorescent Chemodosimeters

Chemodosimetric approach deals with a significant chemical transformation induced by a specific analyte (e.g. cation, anion or neutral molecule). This is an irreversible process and involves with breaking and formation of covalent bonds. The cumulative response originated from the chemical transformation is correlated directly with the concentration of analyte.[40-45] After chemical transformation, fluorescent chemodosimeter produces fluorescence signal that is distinctly different from the initial signal. Usually chemodosimeters have the high selectivity for the target analytes. The disadvantage of this approach is that it needs judicial selection of binding site, signaling unit and specific reactivity. Sometimes slow chemical transformation takes a long time to sense the analyte i.e., it exhibits poor sensitivity.

The above design principles are applied to various organic molecules, polymers, organic-inorganic hybrid materials and nanomaterials to prepare chemical sensors for different neurotransmitters, which are mostly based on the size, shape, electronic properties of neurotransmitters and molecular interactions with the respective materials. A few of them were attempted for the real practical applications in cerebrospinal fluids, serum, plasma and urine. None was attempted in blood platelets, although platelet neurotransmitter (e.g. serotonin) levels are stable index for plasma neurotransmitter concentration. Aptamer conjugated nanoparticles have some prospects because of its high specificity and affinity to specific ligands, but due to moderate binding affinity in some cases it cannot detect lower concentrations. A catalytic and molecular beacon (CAMB) system has very good potential for detecting neurotransmitters due to its sensitivity and analyte specificity. For organic-inorganic hybrid materials, efficiency of the sensor depends on the strength of complexation between specific metal ion and neurotransmitters. In this case, competitive neurotransmitters can affect the detection easily; this is one drawback of this method. Organic molecular sensors require good solubility in aqueous environment, high photo-stability and good quantum yield. Most of the sensors with polymer scaffold are soluble in water, but due to large molecular size, these cannot penetrate the cell membrane easily.

Biogenic Amine Neurotransmitters

Dopamine

Dopamine is a well-known neurotransmitter in mammals.[46] Normal concentration of dopamine in cerebrospinal fluid (CSF) is in the range of 0.5-25 nM.[47] However, it is cardiotoxic at a high level, including high heart rate, death of heart muscles, and high blood pressure.[48] Malfunctions in dopamine-responsive neurons are associated with many diseases such as Parkinsonism, schizophrenia, hypertension,[49] and pheochromocytoma.[50] Thereby, the levels of dopamine or the related catecholamines in biological fluids such as blood or urine are essential indicators in medical diagnostics for the diseases.[51] Electrochemical techniques have mostly been used for its detection in biological fluids.[49]

There have been many efforts to develop a chemical sensor selective to dopamine. Using its strong reactivity to the *o*-phthalic hemithioacetal (OPTA) group,[52-54] dopamine was incorporated into *o*-phthalic hemithioacetal (OPTA)-functionalized mesoporous silicas in a neutral buffer solution to form highly fluorescent (λ_{max} = 440 nm) isoindole through formation of *o*-phthalic hemithioacetal-derivatized materials (Fig. 2).[55] The incorporation was confirmed by ^{13}C cross polarization-magic angle spinning (CP-MAS) nuclear magnetic resonance (NMR) spectroscopy. The selectivity to dopamine over other amines could be modulated by tuning substrate accessibility to the pores through various modification of the surface of OPTA-derivatized mesoporous silica materials. Dopamine takes 10 minutes to complete the reaction whereas glucosamine takes about 2 h, indicating that the reaction is selective to dopamine. A strong dipolar interaction between the hydroxy groups of glucosamine

and the silicates on pore-surface results in its slower diffusion rates within the pores contributing the dopamine selelctivity of the system.

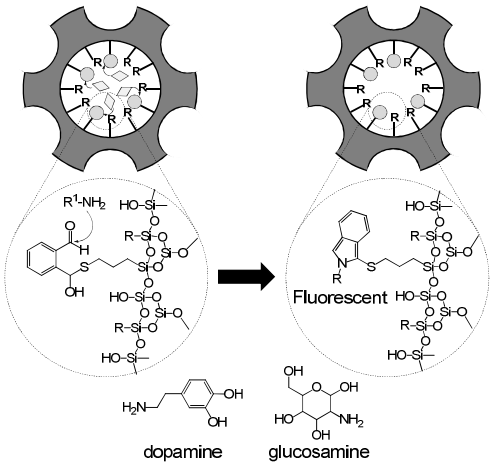

Fig. 2 Schematic illustration of *o*-phthalic hemithioacetal (OPTA)-modified mesoporous silica material for fluorometric measurement of dopamine (R = siloxy, phenyl, propyl, or pentafluorophenyl groups and R'-NH_2 = dopamine or glucosamine).

Raymo *et al.*[56] made use of the electron-rich nature of the dioxyarene fragment of dopamine for fluorimetric detection of dopamine in neutral aqueous environments. They used electron-deficient 2,7-diazopyranium dications to coat the silica particles. The electrostatic interation between dopamine and the dications induces the supramolecular interation of dopamine at the particle/water interfaces (Fig. 3). As a result, the fluorescence intensity of the 2,7-diazapyrenium core **1** at 432 nm decreases dramatically. The fluorescence decay profile at different analyte concentrations indicated that the electron-deficient dications and electron-rich dopamine induce 1:1 and 1:2 complexes at the particle/water interface.

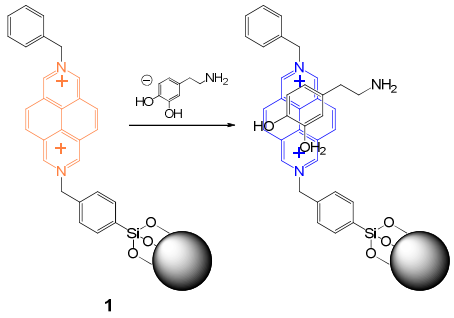

Fig. 3 Silica nanoparticles (NPs) coated with electron-deficient 2,7-diazopyranium dications used in detection of dopamine.

MCM (Mobil Crystalline Materials)- or SBA (Santa Barbara Amorphous)-type of silica are such functionalized silica-based materials. A poly-(lactic acid) (PLA) layer on MCM-41-type mesoporous silica nanosphere (PLA-MSN) material can be used as a gatekeeping unit to regulate the entering of the materials in and out of the nano pores (Fig. 4).[57] Dopamine with OPTA-functionalized PLA-MSN showed significantly higher rate over to those of tyrosine and glutamic acid. This indicates that the PLA-MSN system is very selective to dopamine, over tyrosine and glutamic acid, under the experimental conditions. The difference is due to the large differences of the amine species in their diffusion rates on the nanosphere, caused by the various non-covalent interactions such as H-bonding, electrostatic attractions, and dipolar interactions between these neurotransmitters and the PLA layer under physiological conditions. The isoelectric points of dopamine, tyrosine, and glutamic acid are 9.7, 5.7, and 3.2, respectively, while that of PLA is usually below 2.0.[58] Dopamine carries positive charge while the other neurotransmitters carry negative charge under physiological conditions.

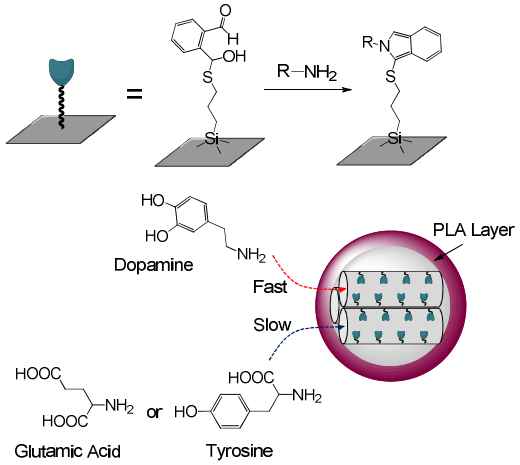

Fig. 4 Schematic illustration of poly-(lactic acid) (PLA)-grafted mesoporous silica nanosphere (MSN) for the detection of dopamine. R-NH_2 indicates the amine-containing neurotransmitter moieties, such as dopamine, glutamic acid, and tyrosine.

Akkaya and Coskun[59] synthesized a fluorescent chemosensor **2** (Fig. 5), which can selectively detect levodopa (L-DOPA), a precursor for the biosynthesis of dopamine *in vivo*, under physiological conditions. They used a lucifer yellow dye (naphthalenedicarboximide), which is water soluble and biocompatible, as well as large quantum yields and Stokes' shift. Moreover, the emission of lucifer fluorophores does not depend on pH in a broad range of pH. Chemosensor **2** has an absorption max at 425 nm and an emission max at 535 nm in 0.1 M MOPS buffer. Increasing concentrations of L-DOPA quenched the fluorescence emission, reducing the intensity to one-fifth of that of the free chemosensor. NMR studies indicated that L-DOPA interacts with the phenylboronic acid moiety. Although the detection of L-DOPA is selective over that of other analytes such as L-phenylalanine, L-tyrosine, and carbohydrates (glucose, fructose, mannose, and galactose), catechol may interfere with the detection of L-DOPA because there are no large differences in the quenching efficiencies of L-DOPA and catechols.

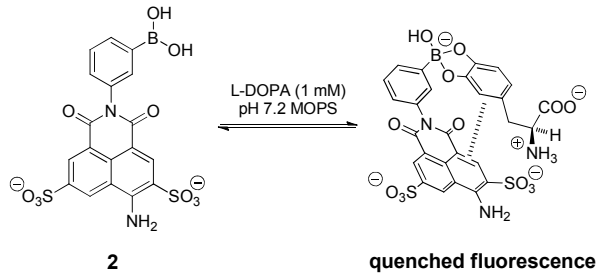

Fig. 5 Proposed chemical structure of sensor **2** and its conjugate with L-DOPA.

Sensor **3** (Fig. 6) exhibited strong binding affinities and selective colorimetric responses to dopamine and norepinephrine even under physiological conditions.[60] It has a coumarin aldehyde scaffold that is suitable for detection of primary amines *via* imine formation. A boronic acid moiety in the scaffold was used as a supporting recognition unit that can enhance both selectivity and affinity for dopamine over other primary amine competitors. A flexible linker placed between the coumarin and boronic acid unit could relieve the structural strains during the complex formation with dopamine. The absorption spectrum of sensor **3** underwent a large red shift (~50 nm) in the presence of dopamine. Glucose and epinephrine failed to show such spectral shift, because these were unable to react with the aldehyde moiety. Moreover, the fluorescence intensity of sensor **3** was decreased upon the addition of dopamine and norepinephrine into the solution. The electron-rich catechol might act as a photo-induced electron transfer (PET) quencher of the coumarin moiety under these conditions. Interestingly, amino acids such as glutamic acid enhance the fluorescence from sensor **3** with 484 nm excitation whereas catechol amines reduce it. Fluorescence titration results indicated a 1:1 binding isotherm with dopamine with a strong affinity (K_a = 3400 M^{-1}). Since epinephrine can bind to sensor **3**, similar to that of norepinephrine, it was concluded that the the strong affinity of sensor **3** to dopamine is contributed mainly by the interactions between the boronate and the bis diol moiety of the catechol.

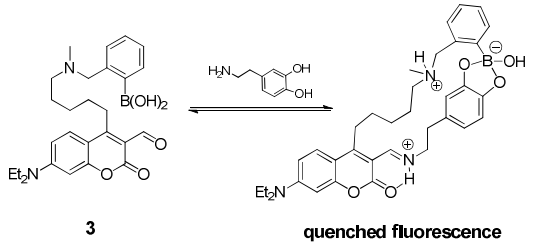

Fig. 6 Proposed chemical structure of sensor **3** and its conjugate with dopamine.

Molecular interactions and surface perturbations can induce conformational transitions, which are associated with distinct color changes (blue to red and vice-versa) and fluorescence transitions, in the "ene-yne"-conjugated polydiacetylene (PDA) backbone.[61-64] The authors combined a phospholipid with PDA to prepare phospholipid/PDA vesicles for the incorporation of synthetic hosts, which are amphiphilic in nature. Receptor **4** recognizes the slim dopamine skeleton.[65] Fig. 7 represents the receptor **4**/phospholipid/PDA assembly where the phospholipid-flanked cavity is accessible to the catecholamine guests for selective binding.

The fluorescence emission (at 560 nm) in the receptor **4**/phospholipid/PDA assembly was occured to surface perturbations induced due to the binding of receptor and catecholamine guests at the water/vesicle interface.[63] The fluorescence emission is proportional to the dopamine concentrations in solution. When the receptor was applied to the urine solutions, a routine sample for diagnostic determination of catecholamines,[66-67] the detection threshold was approximately 1000-fold lower than all currently-available systems that deal with synthetic receptors for the detection of catecholamines.[67] This detection method can be used for the diagnostic applications and screening of catecholamine derivatives.

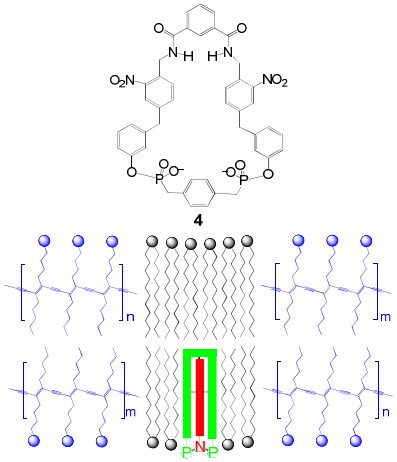

Fig. 7 Chemical structure of macrocyclic receptor **4** and the schematic construction of receptor **4**/phospholipid/PDA assemblies. Blue, PDA; black, phospholipid; green, receptor; and red, ligand.

Raymo *et al.*[69] developed 2,7-diazapyrenium films on glass, quartz, and silica in 1 or 2 steps. Most of the films responded to dopamine at neutral pH in aqueous solutions. The interaction of the 2,7-diazapyrenium acceptors and dopamine donors at the solid/liquid interface induced fluorescence emission quenching. This method is associated with large changes in emission intensity and can be used to detect sub-millimolar concentrations of dopamine. Large concentrations of ascorbic acid did not interfere with the detection.

Cucurbit[8]uril (CB[8]) is a member of the cucurbituril host family and can be used for stable complexation with a 2,7-dimethyldiazapyrenium dication (Me_2DAP^{2+}).[70] The formation of a stable complex between Me_2DAP^{2+} and CB[8] (1:1) was confirmed with ^{1}H NMR spectroscopy, MALDI-TOF (matrix-assisted laser desorption/ionization time-of-flight) mass spectrometry, and X-ray crystallography. Interactions between Me_2DAP^{2+} and electron-rich aromatic guests can form ternary complexes inside the hydrophobic cavity of CB[8]. These ternary complexes have some potential for developing fluorescence-based detection methods for catecholamines and related neurotransmitters (Fig. 8). The absorption spectrum of Me_2DAP^{2+} displayed a decreased absorbance at 245 nm in the presence of the CB[8] host. The fluorescence intensity of Me_2DAP^{2+} at 449 nm (excited at 338 nm) was increased significantly after addition

of 1 equivalent of CB[8]. The Me_2DAP^{2+} can enter into the hydrophobic cavity of CB[8] that shields it from aqueous environment and thus causes fluorescence enhancement. The relative fluorescence intensity of Me_2DAP^{2+} at 449 nm decreased by ~6% in the presence of 1.5 mM dopamine. The decrease is more pronounced in presence of CB[8] (~25% in presence of 1.5 equivalents of CB[8]). The electron deficient $Me_2DAP^{2+}$and the electron rich dopamine can come close to each other in the hydrophobic cavity of CB[8], which drives to static quenching of the excited state of the diazapyrenium dication[71] and thus explains the increased fluorescence quenching of Me_2DAP^{2+}in presence of CB[8]. The appearance of a broad absorption band at longer wavelength (475 nm) supported the charge-transfer interaction between Me_2DAP^{2+} and dopamine in the host cavity.

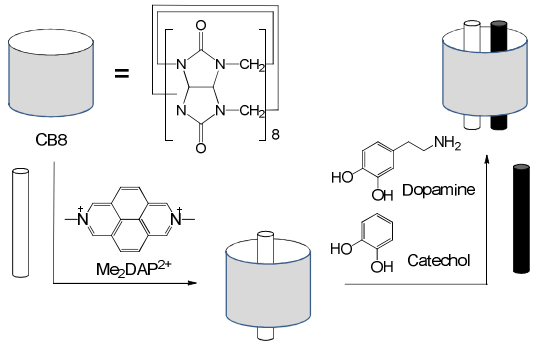

Fig. 8 Schematic representation for the formation of binary and ternary complexes with CB[8].

Poly(*p*-phenylene ethynylene) (PPE)[72] is an amplifying fluorescent polymer with conjugated structures, which is electron deficient and can be used as an excited-state oxidant. Polymer (Fig. 9) has a [2.2.2] bicyclic ring system that shields aggregation-induced self-quenching.[73] The polymer is entirely soluble in water and dimethyl formamide. This can be exploited for detection of amino acids, neurotransmitters, and proteins having electron-donating aromatic moieties in buffers based on PET. The PPE polymer showed a strong absorption band (peak at 405 nm) and strong fluorescence in the blue-green region (432 and 459 nm). Serotonin induced a larger fluorescence decreasement response with polymer than dopamine, as serotonin is a much better electron-donor than dopamine. The K_{SV} (Stern-Volmer) constants for dopamine and serotonin were much higher than those for tyrosine and tryptophan because dopamine and serotonin are positively charged neurotransmitters that help them associate with anionic polymer and the polymer can selectively determine dopamine and serotonine over tyrosine and tryptophan.

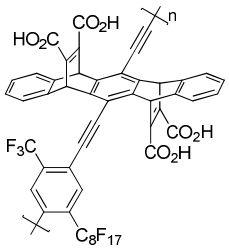

Fig. 9 Chemical structure of poly((*p*-phenylene ethynylene) (PPE).

Tseng *et al.*[74] used phosphate-modified titanium dioxide (P-TiO_2) NPs and fluorescein in aqueous solutions for the selective detection of dopamine, L-DOPA, adrenaline, and catechol. The enediol group of dopamine and of other molecules chelates with surface Ti (IV) ions, which display strong absorption at 428 nm (Fig. 10). This complex may quench the fluorescence emission of fluorescein at 520 nm (excited at 428 nm) when the fluorescein is adsorbed in the particle surfaces. It is noted that excitation at 489 nm (fluorescein absorption band maxima) did not cause fluorescence quenching. The fluorescence emission of a solution of fluorescein containing 1.4 mM P-TiO_2 NPs in buffer (pH 8.0) was decreased with addition of dopamine, L-DOPA, adrenaline, and catechol. The addition of noradrenaline, ascorbic acid, and salicylic acid did not quench the emission. The limits of detection for dopamine, L-DOPA, and adrenaline were 33.5, 81.8, and 20.3 nM, respectively. The authors also detected dopamine in urine samples using the same method.

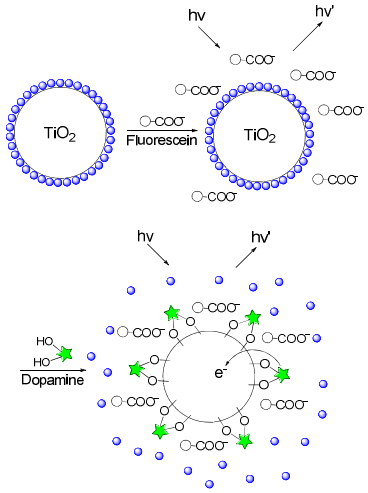

Fig. 10. Schematic representation of the sensing mechanism based on phosphate-modified titanium dioxide (P-TiO_2) NPs and fluorescein. The fluorescence of fluorescein is quenched in the presence of dopamine.

The dopamine unit of **5** (Fig. 11) can bind easily with the boronic acid moiety attached with the quantum dots (QDs) to form a diad system between the QDs and the dye for effective florescence resonance energy transfer (FRET).[75] Upon addition of the dopamine analyte, its competitive binding to the boronic acid moiety to retard the FRET process in a concentration-dependent manner. As fluorescence emission of the dye at 620 nm decreases, the luminescence of the QDs at 570 nm increases, which indicates that the dopamine had bonded with the boronic acid moiety and displaced the fluorescent label. By this method, dopamine was detected with a detection limit of 1 μM. The discrepancy of this method is that it lacks selectivity, since the boronic acid moiety can bind any of the visinal diols.

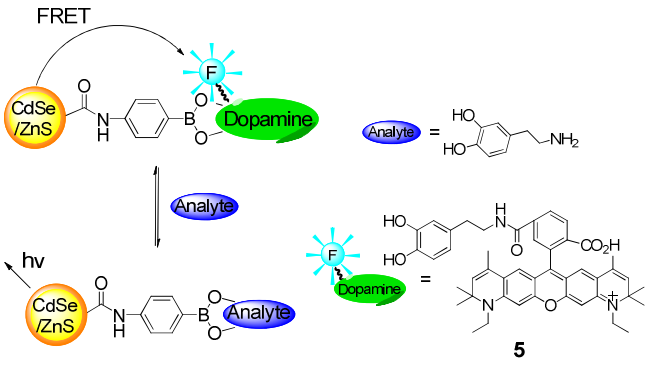

Fig. 11 Competitive analysis of dopamine using fluorophore-labeled dopamine **5**.

Graphene oxide (GO) has good potential as an optical biosensor due to its high mechanical strength,[76] great water dispersibility,[77-78] facile surface modification,[79-81] and high fluorescence-quenching capacity.[82-83] A graphene platform modified with oxygen-containing groups that include hydroxyls, carboxyls, and epoxides improves the water solubility and stability of GO and facilitates non-covalent interactions with diols, amine, and the phenyl group in dopamine due to electrostatic interactions, H-bonding and π-π stacking interactions, enabling detection of dopamine with high selectivity and sensitivity. Addition of dopamine into the solution of GO leads to obvious quenching of GO fluorescence in near-IR region (Fig. 12) at 660 nm, with a blue shift of ~70 nm, which happened within 5 minutes after addition of dopamine.[84] The maximum quenching effect is in the pH range from 4.5 to 7.0, which indicates that there are strong interactions between anionic GO and positively charged dopamine molecules (pI 9.7). The detection limit of this method for dopamine is 94 nM. It has also been successfully applied for the detection of dopamine in biological samples such as urine and blood serum. Very negligible background emission was observed at 660 nm when it was excited at 450 nm in urine and serum samples.

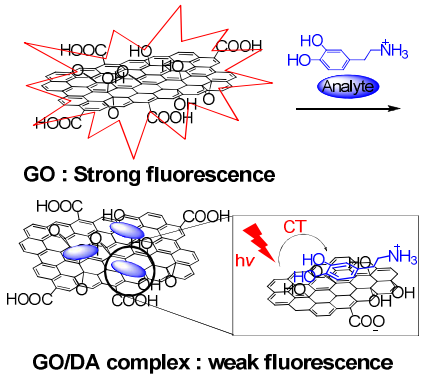

Fig. 12 Schematic depiction for the graphene oxide (GO)-based photo-induced charge transfer fluorescent biosensor for dopamine.

Epinephrine

Epinephrine (also called adrenaline) acts as a hormone as well as a neurotransmitter. As a neurotransmitter, it can regulate smooth muscle contraction and relaxation in skin, lungs, and heart, vasoconstriction in blood vessels, and relaxation of uterus, among other functions. Several analytical methods, such as high performance liquid chromatography (HPLC),[85-87] polarography,[86] and electron-capture gas-LC[87] have been used for the detection of epinephrine. Epinephrine has also been examined by its innate fluorescence due to pre-column derivatization followed by chromatography.[88] Fluorimetric methods are highly rapid and sensitive compare to most conventional techniques, and the determination at parts-per-million to parts-per-billion levels is possible by employing these methods. Some of them, such as the ethylenediamine condensation,[89] terbium(III) fluorescence probe,[90] and trihydroxyindole (THI)[91] methods have been used for the detection of epinephrine.

Yang and coworkers[92] have described an efficient fluorimetric method for the detection of epinephrine. Their system was based on the condensation reaction between epinephrine and formaldehyde. The reaction product was oxidized by potassium hexacyanoferrate (III) ($K_3[Fe(CN)_6]$) in pH 9.5 buffer to make a fluorophore, 6-oxo-4,7-dihydroxy-2-methyl-*iso*-quinoline (ODHMIQ) (Fig. 13). The excess potassium hexacyanoferrate was consumed with ascorbic acid. The excitation and emission band maxima for the system were observed at 428 nm and 498 nm, respectively, in this system. Under optimum conditions, the fluorescence intensity of the system increased gradually with increasing levels of epinephrine in the range of 1.4 nM–2.1 μM. The detection limit was 2.4 nM (signal-to-noise ratio [S/N], 3). Norepinephrine can interfere with the determination of epinephrine by this method. To eliminate this interference, a coupling technique involving synchronous fluorimetry and an H-point standard addition method[93] was used, and the results obtained were satisfactory.

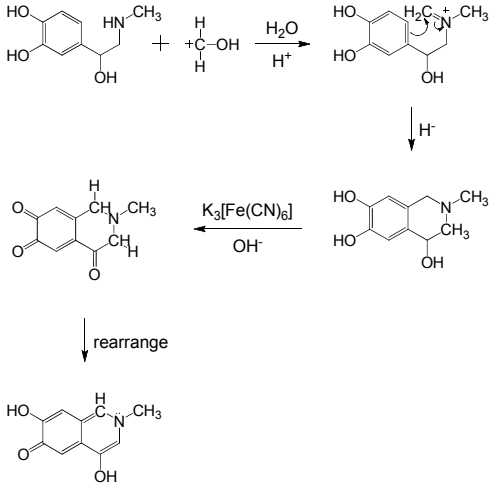

Fig. 13 A fluorimetric method for the determination of epinephrine.

A fluorimetric method based on rare earth columinescence effects of the terbium (Tb)-gadolinium (Gd)-epinephrine-Tris system was established for the detection of epinephrine.[94] In the presence of Gd^{3+}, fluorescence intensity of the epinephrine-Tb^{3+} system was increased and excitation peak was moved towards shorter wavelengths (from 325 nm to 300 nm). After subsequently adding Gd^{3+} to the Tb^{3+}-epinephrine-Tris system, the emission of epinephrine was gradually weakened and that of Tb^{3+} was gradually enhanced. The energy absorbed by

epinephrine was moved to the Tb^{3+} complex through the oxygen bridge, which resulted in fluorescence enhancement. Enhancement of fluorescence also originated from the energy-insulating sheath of Gd^{3+} surrounding the Tb^{3+} complex as the seath might prevent collisions with water molecules and reduce the energy loss of the Tb^{3+} complexes. The mechanism was supported by fluorescence lifetime measurements of Tb^{3+} in different systems. Upon addition of epinephrine to the Tb^{3+}-Tris system, the fluorescence lifetime of Tb^{3+} was delayed from 6.86 to 32.35 ns. Upon addition of Gd^{3+} to the Tb^{3+}-E-Tris system, the fluorescence lifetime of Tb^{3+} was tremendously prolonged from 32.35 to 1807 ns. A linear relationship of fluorescence intensity regarding epinephrine concentration was obtained in the range of 18 to 2.5 μM under optimum conditions. The detection limit was 4.5 nM (S/N, 3). It has also been successfully applied for the detection of epinephrine in biological samples such as urine by the standard addition method. The limitation of this method is that norepinephrine, dopamine, and proteins interfere considerably with the detection of epinephrine.

Epinephrine in human serum was detected by a very rapid, simple, and susceptable fluorimetric technique, which exploited the endogenous fluorescence of epinephrine.[95] The absorption and emission band maxima of epinephrine in aqueous buffer solutions were located at 286 and 360 nm, respectively. The efficiency as well as sensitivity of this method depend entirely on the optimization of experimental parameters, such as pH, temperature, concentration of anionic surfactant etc. The proper selection of excitation and emission wavelengths is also important to regulate the efficacy of this method. The measurement was carried out at 360 nm with excitation at 286 nm. A linear correlation was obtained between the fluorescence intensity and epinephrine concentration in the range of 0.10 and 1.0 μg/mL under optimum experimental conditions. The detection limit was 0.05 μg/mL. A recovery test carried out with known amounts of epinephrine in human serum indicated an efficiency of 95.5–98.7%.

Norepinephrine

Norepinephrine (also called noradrenaline) acts as a hormone as well as a neurotransmitter. The structural difference between epinephrine and norepinephrine is only that epinephrine has a methyl unit connected to its nitrogen, while a hydrogen atom is substituted in place of the methyl unit in norepinephrine (Fig. 1). Norepinephrine is released from noradrenergic neurons in the CNS (central nervous system) and sympathetic nervous system and has been closely associated in some physiological processes such as anxiety, stress, sleep, and memory. The abnormal levels of norepinephrine in plasma and urine are utilized as a biomarker for several diseases such as hypertension, pheochromocytoma, and neuroblastoma. Many methods for the determination of norepinephrine have been reported in different media with high sensitivity and precision.[96-100] Most recently-used methods in clinical research utilize HPLC (high performance liquid chromatography) connected with electrochemical detection. However, none of these methods is completely specific or have sufficient sensitivity.[98] Several fluorimetric methods for catecholamines, based on native fluorescence, have been described, such as synchronous and derivative spectrofluorimetry-based,[101] ethylenediamine condensation-based, and trihydroxy indole-based methods.

The oxidation of catecholamines like epinephrine and norepinephrine produces aminochrome derivatives, the levels of which can be examined spectrophotometrically at 486 nm (absorption band maxima).[102] Sodium bismuthate can be used as a sensitive chromogenic moiety and potential oxidant in pH 3 aqueous medium. Bismuthate develops red coloration after being reduced. The optical density at 486 nm was linear with the concentration of norepinephrine (or epinephrine) in the level range of 4.8–600 μM. The detection limits was 2.46 μM for norepinephrine. The method was successfully applied for the determination of norepinephrine (or epinephrine) bitartarate in pharmaceutical formulations.

Intramolecular FRET technique in combination with LC has been used for the determination of catecholamines.[103] In this approach, native fluorescent bioamines (indolamines and catecholamines) are derivatized with a fluorophore, *o*-phthalaldehyde (OPA). Native fluorescent bioamines act as donors and the derivatized fluorophore acts as an acceptor in this FRET-diad system. When the OPA derivatives of the native fluorescent bioamines were excited at absorption maxima of the native fluorescent bioamines (280 nm), these emited OPA fluorescence (445 nm) through an intermolecular FRET process. In conventional fluorescence studies, OPA derivatives were excited at 340 nm and emission band maxima was at 445 nm. OPA derivatives of the indolamines and catecholamines were successfully performed when seperating LC on an ODS column. The detection limits (S/N, 3) for the indolamines and catecholamines, at a 20-μL injection volume, were 17–120 and 28–200 fmol, respectively.This method also provided enough selectivity and sensitivity for the detection of the indolamines in the human urine sample. The detection limits (per 20-μL injection volume; S/N, 3) of the natively-fluorescent bioamines (while FRET derivatization was used) were in the range of 17–200 fmol.

Norepinephrine was oxidized by mercury (II) nitrate. The oxidized product was reacted with ethylenediamine to form a strong fluorescent compound (Fig. 14).[104] The measurement of fluorescence intensity was carried out at 507 nm, exciting at 420 nm. A linear relationship of the fluorescence intensity regarding norepinephrine concentration was observed in the range of 0.01 μM–0.014 mM. The detection limit was 2.5 nM. The interference from dopamine was removed by the first derivative synchronous fluorimetric system using the peak-to-zero technique. The results of recovery efficiency test in urine samples indicated a 95–98.62% recovery. The method was also successfully applied to the detection of norepinephrine in injection solutions.

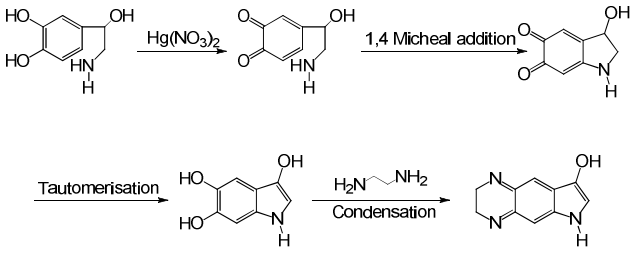

Fig. 14 Reaction pathway of norepinephrine for the formation of the condensation product.

Serotonin

Serotonin plays a regulatory role in the modulation of various cognitive and behavioral functions such as sleep, mood, pain, depression, anxiety, and learning by binding to many serotonin receptors present on the cell surface.[105] In biological systems, many tryptophan derivatives (Fig. 15) such as 5-methoxyindoleacetic acid, 6-hydroxymelatonin, melatonin, serotonin, 5-methoxytryptamine, and 5-hydroxytryptophan have been discovered.[106]

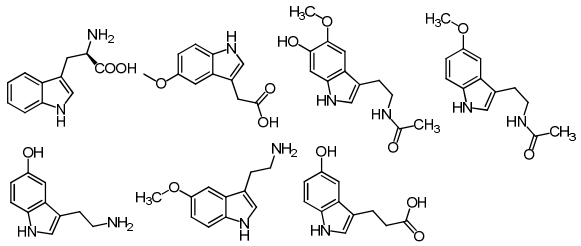

Fig. 15 Various biological derivatives of tryptophan.

Normal serotonin levels in CSF, plasma are in the range of 93-902pg/ml and 1.37-4.44ng/ml respectively. It is 528±137ng/10^9 blood platelets[107].

In various analytical methods for serotonin, other monoamines, including histamine, dopamine, norepinephrine, and epinephrine, have similar reactivity to that of serotonin and, in particular, indole-containing monoamines have similar fluorescence properties. The intrinsic fluorescence of serotonin originating from its indole moiety can be used for its analysis.[108] The absorption and emission maxima of serotonin are located at 337 and 297 nm, respectively. The spectroscopic properties of serotonin such as fluorescence, emission maximum, and lifetime are pH-dependent, consistent with a p*Ka* of 10.4 ± 0.2. At pH values higher than its p*Ka*, the fluorescence emission of serotonin is quenched.

To investigate serotonin in biological systems, its intrinsic fluorescence was measured under various experimental conditions. The simplest example may be application of fluorescence LC.[109] Serotonin levels were analysed using HPLC (aqueous citric acid buffer mobile phase; 5-Am C18 column with fluorescence detection, 280/340 nm) in homogenized planaria responding to dopaminergic ligands, such as cocaine and opioids, by using N-methyl-5-hydroxytyrptamine (HT) was used as an internal standard. The detection limit of the procedure was 0.35 ng.

A CE method with detection of native fluorescence of analytes based on a micellar electrokinetic chromatography method has been introduced for synchronous detection of melatonin and its precursors and metabolites such as tryptophan, 5-methoxyindoleacetic acid, 6-hydroxymelatonin, melatonin, serotonin, and 5-methoxytryptamine.[106] A pH 9.5 buffer system (borate 20 mM) containing SDS (50 mM) served as the electrolyte. The limits of detection were at the sub-ppm level.

A label-free determination method based on detection of the native fluorescence from serotonin and its related compounds in less than 1 min was reported based on microchip electrophoresis (MCE), with excitation at 266 nm.[108] In bananas, after 10 days of ripening, the concentration of serotonin was measured to be 2.7 μg/mL through quantitative analysis of the extracts.

The native fluorescence of serotonin requires UV light for excitation; therefore, excitation with 2 or multiple photons using visible light would be better. Two-photon fluorescence method at 420 nm for label-free detection of serotonin in microchip electrophoresis was presented in a recent report.[111] The detection limit was in the μM range, utilizing excitation light of 420 nm.

Stronger fluorescent properties can be generated from simple chemical modifications of serotonin. Derivatization of serotonin with benzylamine or 1,2-diphenylethylenediamine (DPE) followed by column LC was introduced in 1 study.[112-113] The derivatization was initiated with benzylamine or DPE in basic media (pH 10.0), where potassium hexacyanoferrate (III) plays a catalytic role according to the reaction mechanisms shown in Fig. 16. The resulting fluorescent benzoxazole moieties were separated on a reversed-phase column. By this method, serotonin was detected with a detection limit of 0.08 fmol per 20-μL injection (12 pM in a standard solution).

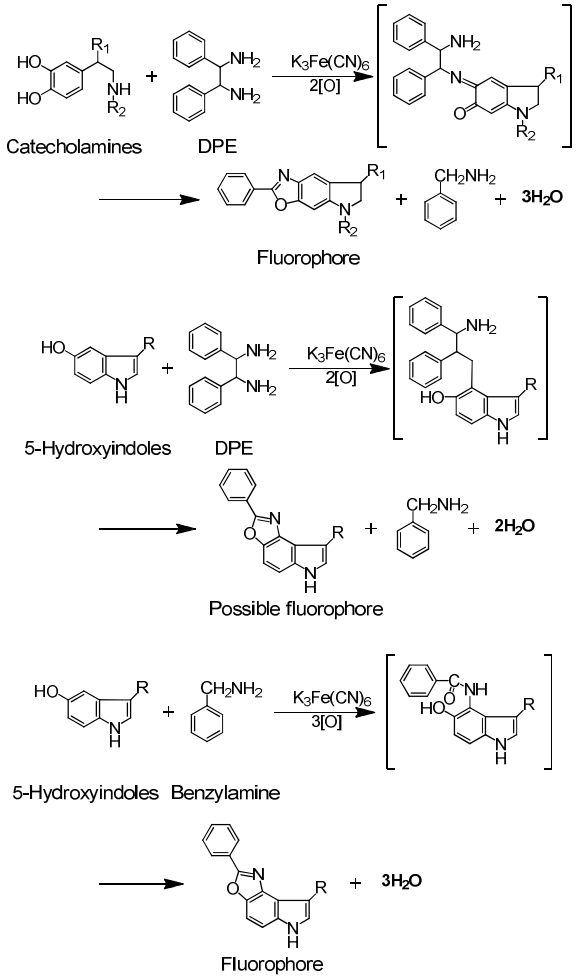

Fig. 16 Fluorescence derivatization procedure for 5-HT and 5-hydroxyindoleacetic acid using 1,2-diphenylethylenediamine and their sensitive liquid chromatographic detection.

The levels of serotonin (expressed in μg/g wet weight, mean ± S.E.M, n = 5) in tissue extracts from the rat striatum was evaluated to be 0.45 ± 0.05.[110-111] This modification generates good linearity up to 1 pmol of serotonin and the relative standard deviation for repeated analysis (n = 10) of serotonin at levels of 50 fmol/20 μL was 4.2%. In a buffer solution of pH 5.80 (NaAc-HAc), serotonin can react with the formaldehyde-acetylacetone system, which then followed by a new compound to give yellow-green fluorescence at 533 nm, and enhancement of fluorescence intensity regarding the concentration of the newly formed 5-HT was observed.[114] The detection limit for the detection of serotonin with this method is 2.08×10^{-7} mol/L. This newly developed method can be successfully applied to the analysis of serotonin in biological fluids, such as human urine and serum samples. The mechanisms underlying fluorescence enhancement in the serotonin-formaldehyde-acetylacetone system follows the Hantzsch reaction (Fig. 17), where the serotonin reacts with acetylacetone-formaldehyde, which then followed by a new ternary complex to give a marked fluorescence enhancement of the acetylacetone-formaldehyde complex at λ = 533 nm. Enhancement of fluorescence intensity regarding the concentration of the newly formed 5-HT was observed.

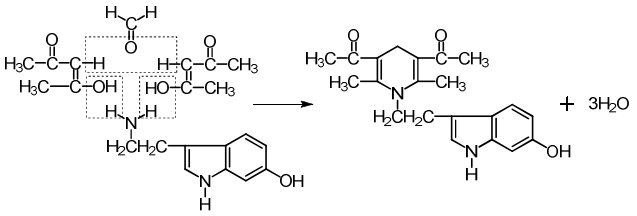

Fig. 17 Hantzsch reaction in the serotonin-formaldehyde-acetylacetone system.

The method has poor selectivity for serotonin over the other amines, amino acids, proteins and other substances. However, the extraction and re-extraction methods were used to improve the selectivity[115].

A traditionally important modification of amine with fluorescein isothiocyanate isomer I (FITC) is also applied to serotonin detection, which was demonstrated with a CE-laser-induced fluorescence (CE-LIF) method.[116] An argon ion laser of 488 nm and a 520 nm band-pass emission filter were employed. A linear relationship of fluorescence intensity was obtained in the range of 0 and 188 nM under optimum conditions. The detection limit was 16 nM and an RSD (relative standard deviation) between 2% and 9%. The system was successfully applied to analysis of 5-HT in human urine samples.

The intramolecular excimer-forming fluorescence derivatization with 4-(1-pyrene)butanoyl chloride is also a clear example of fluorescent derivatization for serotonin detection,[117] which has been demonstrated by reversed phase LC. Polypyrene-labeled derivatives sensitively sense the amino and phenolic hydroxyl functional parts in serotonin, which then followed by intramolecular excimer fluorescence (Fig. 18) to give a discriminated fluorescence from reagent free. The detection limits (S/N, 3) for catecholamines and indolamines were at fM levels per 20-μL injection volumes. The system was successfully applied to a urine assay, indicating its utility for assaying serotonin in biological samples.

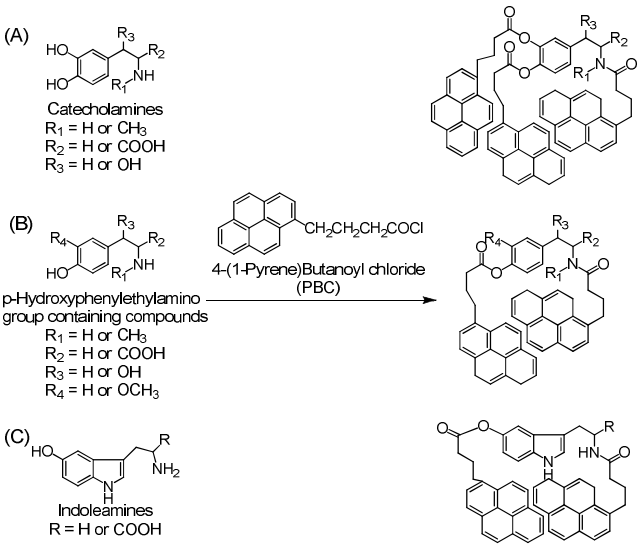

Fig. 18 Intramolecular excimer-forming fluorescence derivatization of bioactive amines with 4-(1-pyrene)butanoyl chloride. Amines: (A) catecholamines; (B) *p*-hydroxyphenylethylamino group containing compounds; and (C) indolamines.

Intramolecular FRET detection was applied in an LC system, which has been followed precolumn derivatization of serotonin's amino groups (Fig. 19).[118] The FRET occured from the native fluorescent moieties (donor) to the derivatized fluorophore (acceptor) in this system. Among 15 fluorescent reagents, *o*-phthalaldehyde (OPA) was the most efficient in generating the FRET from a screening study, which followed by an intermolecular FRET process by excitation of the native fluorophore (280 nm) to give OPA fluorescence (445 nm). In separation of the derivatized serotonin in LC on an ODS column, the detection limits (S/N, 3) were 17–120 and 28–200 fmol per 20-μL injection volumes, respectively. Furthermore, this system was successfully applied to a urine assay, indicating its utility for the determination of the indolamines.

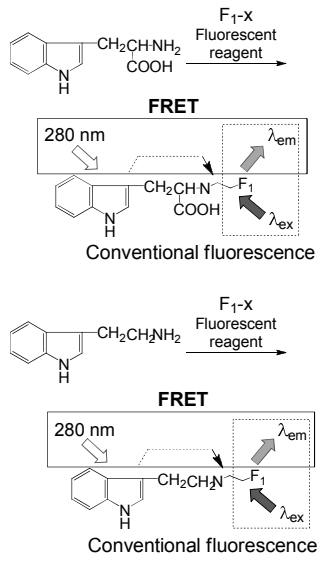

Fig. 19 Intramolecular FRET detection of tryptophan and dopamine.

Detection of serotonin using a charge-transfer complex between the attached viologen moieties was demonstrated with a thin solid film composed of a hyperbranched viologen polymer.[119] 4-(*N*-methoxyethylpyridiniumyl)-4′-pyridine was prepared by coupling 4-4′-bipyridine and p-toluenesulfonic acid 2-isopropoxyethyl ester and then reacted with HBPS-Br to produce **7** (Fig. 20). Although the charge-transfer spectroscopic changes observed red shifts with increasing donor fractions only in the case of a thin solid film composed of a hyperbranched viologen polymer, this system is sensitive enough to detect serotonin at the 2 μM level even in the presence of L-tryptophan.

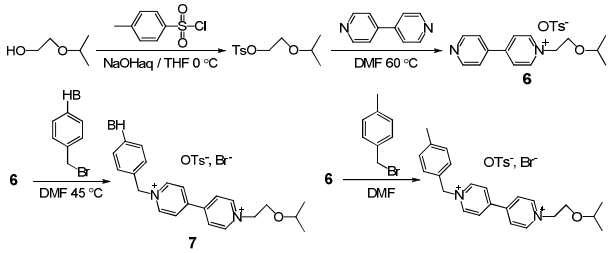

Fig. 20 Synthetic scheme of a hyperbranched viologen polymer **7**.

On the basis of the supramolecular interaction with cyclodextrin (CD), serotonin in urine was determined fluorimetrically.[120] The dicationic guest 2,7-dimethyldiazaphenanthrenium ((DPT^{2+}) forms a fluorescent inclusion complex with the CB[8] host (Fig. 21), which can be used to effectively bind and detect indole derivatives, such as serotonin and tryptophan.[121] CB[8] is capable of hosting 2 suitable aromatic guests and form stable ternary inclusion complexes. In order to retain enough volume for an additional π-electron donor guest within the cavity, a 2,7-dimethyldiazaphenanthrenium (DPT^{2+}) dication was prepared. After preparation of the DPT^{2+}@CB8 complex as the fluorescent receptor for indole, tryptophan and serotonin were presented. A strong fluorescent emission was observed (λ_{em} = 405 nm), as anticipated from the rigid character of the aromatic region of this dication in the DPT^{2+}-CB[8] complex, but the emission is strongly related to the charge transfer bands resulting from the strong interaction between the π-electron acceptor guest (DPT^{2+}) and the π-electron donor guest (indole derivative) inside the CB[8] cavity. The K_a value for indole is (1.1 ± 0.2)×10^6 M^{-1}. Similarly, the values for tryptophan and serotonin were (4.2 ± 0.1)×10^5 M^{-1} and (1.4 ± 0.1)×10^5 M^{-1}, respectively.

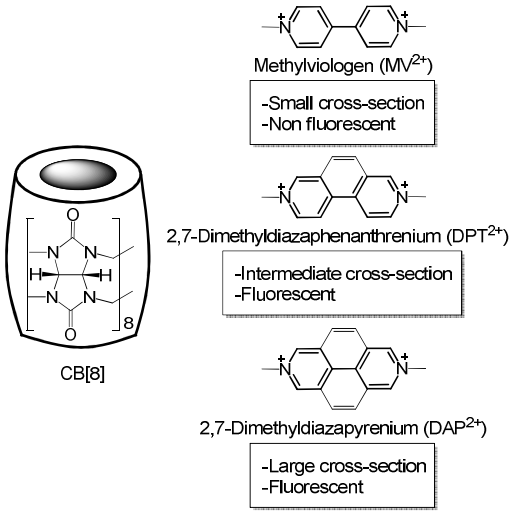

Fig. 21 Structures of the cucurbit[8]uril host and various electron acceptor guests.

Histamine

Histamine (2-(4-Imidazolyl)-ethylamine) is an aminergic neurotransmitter. Histamine is synthesized by decarboxylation of the amino acid L-histidine in a reaction catalyzed by the enzyme histidine decarboxylase. It is involved in several brain-related functions such as food intake, memory formation, sleep, hormonal secretion, thermoregulation, cardiovascular control, regulation of immune function, inflammation, gastric acid secretion, and neuromodulation. The normal concentration ranges of histamine in CSF, plasma and urine are respectively 388.05±51.19 pmol/ml, 39.19±20.22 pmol/ml and 182.4±126.4 pmol/mg.[122-123] Histamine imbalance in the body is associated with abnormal arousal, Alzheimer disease, and other neuropsychiatric disorders.

Yamaguchi *et al.*[124] devised a simple but highly-sensitive and selective method for the detection of histamine by HPLC coupled with fluorescence determination. The method was based on intramolecular excimer formation of a histamine derivative (Fig. 22) prepared with histamine and 4-(1-pyrene)butyric acid *N*-hydroxysuccinimide ester (PSE). Since histamine has 2 amino moieties in a molecule, it can be facilitated to a dipyrene-forming derivative in the presence of PSE. The derivative displayed excimer fluorescence in the wavelength range of 450 to 540 nm in acetonitrile, which can be easily distinguished from the monomer emission of PSE in the wavelength range of 370 to 420 nm. For a 30 μL injection in the HPLC instrument, the detection limit (S/N, 3) of histamine was 0.5 fmol. The device was

successfully applied to the histamine determination in human urine samples.

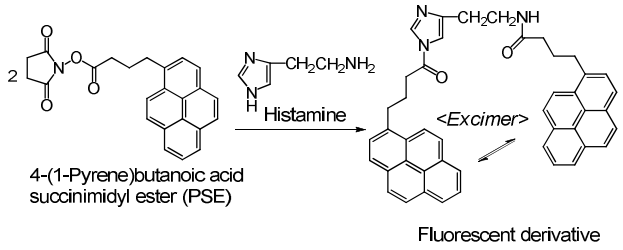

Fig. 22 Schematic representation of the derivatization of histamine with 4-(1-pyrene)butyric acid *N*-hydroxysuccinimide ester (PSE).

A ligand exchange method was exploited for the efficient determination of histamine in buffer solution (0.1 M phosphate buffer solution, pH 7.4).[125] The sensor was devised with a calcein **8**- Ni^{2+} complex. Calcein **8** is a fluorescein moiety that consists of 2 iminodiacetic acid parts, and its fluorescent emission is quenched due to the binding of several metal ions, including Ni^{2+} with iminodiacetic acid units (Fig. 23). Upon addition of histamine to a solution of **8**- Ni^{2+}, the Ni^{2+} ions in compound **8**-Ni^{2+} sensitively senses histamine, which followed by exchange to form a histamine-Ni^{2+} complex, which suppressed the fluorescence quenching by Ni^{2+} ions, resulting in the recovery of the fluorescence emission (at 515 nm) from the calcein moiety. The sensor was very selective for histamine, over other neurotransmitters such as dopamine, GABA, glycine, glutamic acid, and serotonin. The method was also applied for the histamine determination produced by RAW264 cells *in vivo*.

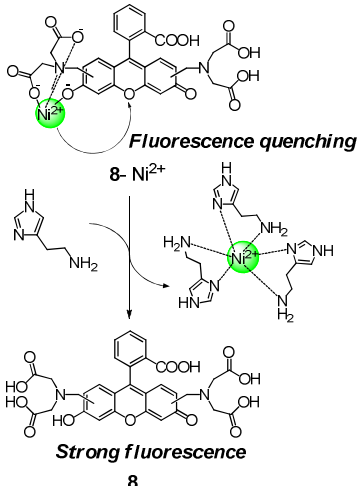

Fig. 23 Schematic illustration of the sensing mechanism of histamine using **8**-Ni^{2+}.

Imato *et al.*[126] demonstrated the imaging of histamine in living cells (RAW264 cells) using Nile red as the fluorescent probe. The dye **9** was modified with an iminodiacetic acid moiety that can bind Ni^{2+} and cause fluorescence quenching of Nile red. The probe (with hydrophobic and hydrophilic units) was designed in such a way that it had an amphiphilic character and water solubility, allowing it to penetrate the cell membrane. As discussed before, in presence of histamine, histamine coordinates with Ni^{2+} and the coordinated ions are dissociated from the probe, which restores the fluorescence of Nile red (at 670 nm, when excited at 600 nm) (Fig. 24). This method was also very selective for histamine over other neurotransmitters, amines, and thiols. The method is less selective over glycine, putrescine, glutamic acid and glutathione, if the Cu^{2+} complex is used.

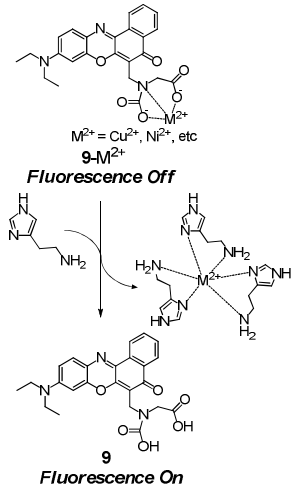

Fig. 24 Schematic illustration of the sensing mechanism of histamine using **9**-M^{2+}.

A heterobimetallic Ru(II)-Eu(III) complex was used as a colorimetric and luminescent sensor **10** for the selective determination of biogenic amines in fish samples.[122] Chemodosimeter **10** (Fig. 25) was synthesized by Chow, Lam, and coworkers.[127] When histamine was added to the ethanolic solutions of **10**, the metal-to-ligand charge transfer (MLCT) transitions of the complex were shifted from 417 to 435 nm and the MLCT emissions were shifted from 644 to 654 nm with significantly enhanced intensity. The chemodosimeter was not selective for a particular biogenic amine. However, only the analytes with an aliphatic amino functionality (histamine, putrescine, spermidine, and ammonia) enabled to induce the fluorescnece responses. Other common moieties containing aromatic amino functionalities were not able to show any observable fluorescence changes. The detection limit was estimated to be 10 ppb.

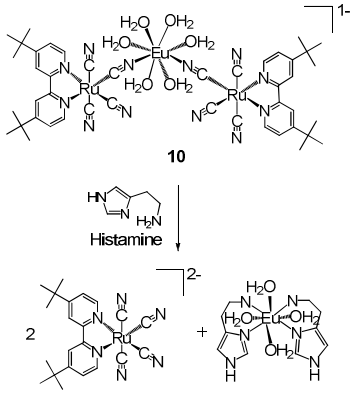

Fig. 25 Proposed molecular recognition and luminescence signaling mechanism for the determination of histamine.

Acetylcholine

Acetylcholine (ACh) is a polyatomic cation, which is an ester of acetic acid and choline (Fig. 26) and plays a significant role as a neurotransmitter in both the peripheral and central nervous systems. The role of Ach in the peripheral nervous system includes the control of muscular contraction, ganglionic transmission, inhibition effects in the ion channels by Ach receptors. It is also associated with the regulation of temperature and blood pressure, memory and learning. Several diseases are linked to cholinergic malfunctions, such as coronary artery disease, aging-related changes in cognition, and Parkinson disease.[128]

Many analytical methods have been developed for the measurement of Ach and choline (Ch), which include gas chromatography (GC) with flame ionization detection, GC with mass spectrometry (GC-MS), LC with electrochemical detection (ED), and bioassay methods. Various types of biosensors have also been devised based on co-immobilized enzymes.[129-136] Each technique has its own limitations, such as poor selectivity and sensitivity. GC-MS and LC-ED techniques require expensive instrumentation, and sophisticated sample clean up and extraction systems. The ED method with co-immobilized enzymes is more attractive, but it is not as sensitive for precise monitoring ACh/Ch levels in blood samples. Moreover, the above methods are limited to the detection of ACh and Ch *in vivo*, especially in nervous tissue. A chemiluminescense (CL) method has been developed to assay Ach in the brain.[137]

p-Sulfocalix[*n*]arenes (**11-14**) is water soluble and can form complexes with the chromophore *trans*-4-[4-(dimethylamino)styryl]-1-methylpyridinium-*p*-toluenesulfonate (**15**).[138] The free chromophore (50 μM) exhibited a weak fluorescence at 604 nm in a PBS/MeOH solution (pH 7.2). The stepwise addition of **13** solution into the solution of **15** resulted in a gradual increasement of emission intensity, which was ~30-fold higher than the initial intensity of the free chromophore **15**. The emission band was shifted by ~34 nm toward a shorter wavelength (bathochromic shift). The presence of ACh can displace the chromophore molecules from the calixarene cavity and the emission band of the free chromophore **15** reappears. Fluorescence, ^{1}H NMR, and UV-Vis absorption spectroscopy were utilized to study the formation and dissociation of the complex. ACh can be selectively detected by the *p*-Sulfocalix[*n*]arene-**15** complex in solution with a detection limit of 50 nM. The binding of ACh with *p*-sulfocalix[*n*]arenes was based on electrostatic and hydrophobic interactions between the cationic quaternary ammonium terminus and the electron-rich *p*-sulfocalix[*n*]arene.[139-140] Moreover, it was observed that monocarboxyl *p*-sulfocalix[4]arene immobilized onto a silicon surface can form complexes with the chromophore (**15**) and subsequently enable detection of ACh in solution. This can help in the development of a solid state-based optoelectronic biosensor for ACh.

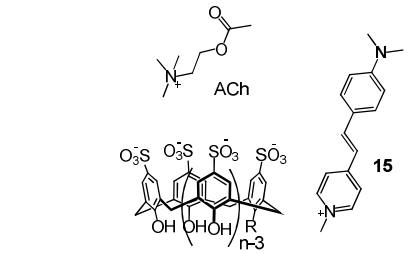

11: n=4, R=OH **12**: n=4, R=OCH$_2$COOH
13: n=6, R=OH **14**: n=8, R=OH

Fig. 26 Molecular structure of *p*-sulfocalix[*n*]arenes (**11-14**), chromophore (**15**), and ACh.

Tang *et al.*[141] used hydrogen peroxide (H_2O_2)-sensitive QDs to construct a biosensor that can detect ACh sensitively. The detection method was based on the fluorescence quenching of the QDs by H_2O_2, which was produced from an enzymatic reaction from ACh. Acetylcholinesterase (AChE) catalyzed the conversion of ACh to choline, and choline oxidase (ChOx) diffused to the surface of the CdTe QDs and catalyzed the production of H_2O_2 from choline (Fig. 27). H_2O_2 underwent an electron transfer (ET) process with the CdTe QDs, thereby quenching the fluorescence of the QDs. When the Ach concentration was increased, fluorescence intensity of QDs was quenched gradually. The detection limit for ACh was found to be 10 μM and the linear range was 10–5000 μM. The detectable linear range and recovery of ACh in serum samples was 10–140 μM and ~99%, respectively.

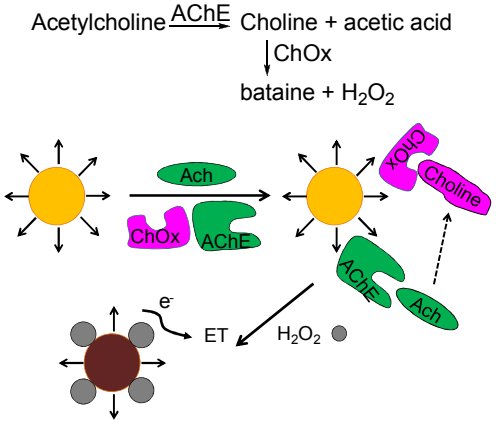

Fig. 27 Schematic illustration for the ACh assay using a biosensor.

Amino Acid Neurotransmitters

Glutamate

Glutamic acid is a non-essential amino acid. The carboxylate anions or salts of glutamic acid are known as glutamate, which is used as a major excitatory neurotransmitter in the mammalian CNS. It is involved in most aspects of normal brain functions including memory, cognition, learning, and perception of pain. The normal concentration of glutamate in the extracellular fluids of brain is low (in the micromolar range). The glutamate concentration inside neurons of the brain is several thousand times higher (~1–10 mM). Glutamate imbalance is harmful to human health, as it is implicated in several neurological diseases

associated with glial and neuronal death.[142-146]

Recently, Bhuyan *et al.*[147] reported a series of water-soluble triazine bis-Zn^{II}-cyclen complexes with rigid structures for the recognition of phosphate anions and non-covalent protein labeling in buffer solution (Fig. 28). In HEPES buffer (25 mM, pH 7.4), upon addition of oligoaspartate (D_4-tag) and oligoglutamate (E_4-tag) tags to a solution of the tetra-Zn^{II} complex **16d**, the fluorescence (~6.8 and ~4.8 fold, respectively) signal was enhanced. Fluorescence spectroscopic analysis and density functional theory (DFT) calculations, along with analysis of the binding isotherms, showed that complex **16d** was most selective for both the oligoglutamate (E_4-tag) and oligoaspartate (D_4-tag) tags, with stepwise binding constants of ca. 10^7 M^{-1} because of the enhanced coulombic interaction in the host-guest complex.

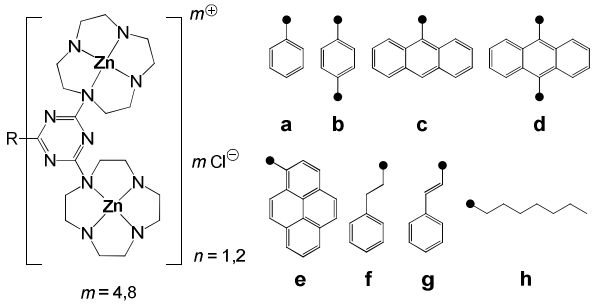

16

Fig. 28 Structures of triazine bis-Zn^{II}-cyclen complexes **16a-h**.

Wang *et al.*[148] synthesized bis(indolyl)methane **17**, which contains a conjugated bisindole skeleton. It is a highly selective and sensitive chromogenic-sensing molecular model based on the proton transfer signaling mode (Fig. 29). In CH_3CN/H_2O (1:1, v/v) solution, o.nly aspartic acid and glutamate selectively induced a yellow-to-red color change. The changes in color and absorption spectra (peak shifts from 435 nm to 500 nm) may have originated from the proton transfer from the acids (Asp or Glu) to **17**, which may modulate the internal charge transfer in the protonated receptor. The detection limits for Asp and Glu were 0.80 and 1.12 ppm, respectively.

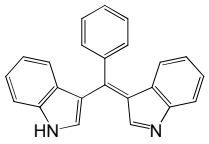

17

Fig. 29 Structure of bis(indolyl)methane **17**.

Doong *et al.*[149] developed a silica sol-gel-grafted array-based biosensor that can sense potential biomarkers for Alzheimer disease, including β-amyloid, ACh, and Glu; it can also detect H_2O_2 and the pH. The biosensors displayed good performance on simultaneous analysis of multiple analytes without any cross-interference. The detection limits of H_2O_2, β-amyloid, Glu, and ACh were 1.57, 0.63, 0.55, and 1.0 μM, respectively. The applicability of array biosensors was successfully demonstrated for the detection of β-amyloid and related metabolites in spiked human serum samples.

Guan *et al.*[150] developed a sensitive method based on a polythiophene (PT)-AgNPs system for sensing Asp and Glu (Fig. 30). The emission peak of PT appeared at 514 nm, which had a spectral overlap with the absorption of gold NPs (AuNPs), which have a peak at 510 nm. This caused dramatic fluorescence quenching of PT by AuNPs through a highly-efficient energy transfer process. In aqueous solutions, AuNPs were displaced from the PT surface after addition of 2 acidic amino acids, Asp and Glu, due to the formation of H^+-AuNPs, which, in turn, leads to the restoration of the fluorescence of PT. The fluorescence enhancement from the AuNP-PT system can quantitatively reflect the amounts of adding Asp or Glu, when the fluorescence intensity at 514 nm is monitored. A good linear relationship was obtained in the concentration range of 7.5×10^{-8} to 6×10^{-6} M and 9.0×10^{-8} to 5×10^{-6} M, respectively, for Asp and Glu. The limits of detection were 32 and 57 nM, respectively, for Asp and Glu (S/N, 3). The system was successfully applied to biological samples collected from a fine chemicals factory.

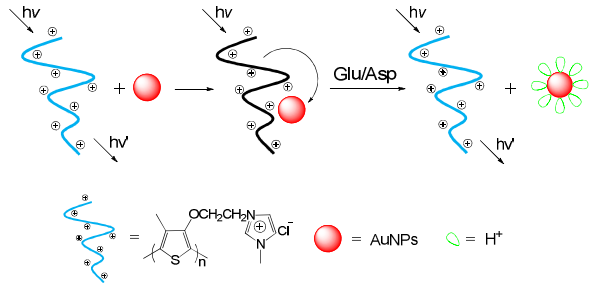

Fig. 30 Schematic illustration of the ''turn-on'' fluorescent sensing for Glu/Asp based on the PT-AuNP system.

Chadlaoui *et al.*[151] reported a triazolopyridine-based fluorescent sensor for the determination of metal ions, anions, and amino acids (Fig. 31). In ethanol, the binding of the triazolopyridine derivative to Zn^{2+}, based on π-conjugation, led to fluorescence quenching, as well as an intensity decrease in the absorption band at 373 nm and the occurance of a new band at 382 nm. Addition of amino acids such as Asp and Glu produces a recovery of the emission intensity at 464 nm similar to that of **18**.

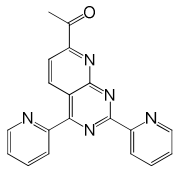

18

Fig. 31 Structure of chemosensor **18**.

A cholic-acid-based fluorescent receptor for determination of dicarboxylate anions and amino acids have been developed in a 1:1 CH_3OH/buffer co-solvent system (0.01 M HEPES, pH = 7.4) by Liu *et al.*[152] (Fig. 32). Upon addition of L-Asp, Glu, *N*-acetyl-L-Asp and *N*-acetyl-L-Glu, the fluorescence intensity of **19** can be quenched by ca. 20%. On the basis of the change of fluorescent intensity, the association constants (K_a) were measured using nonlinear least-squares curve fitting. Such

analyses revealed that the preorganization of **19** permits 3-point binding with the guests, following by a more selective complexation with acidic amino acids than their corresponding dicarboxylates; moreover, **19** strongly binds Glu through multiple hydrogen bonds, with a binding constant of (5.57 ± 0.88) × 10^6 M^{-1}.

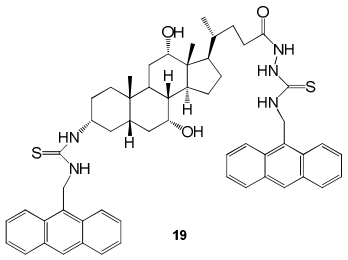

Fig. 32. Structure of probe **19**.

Issberner *et al.*[153] reported a chemosensor for determination of the localized L-Glu release at the neuromuscular junction in insects (Fig. 33). An L-Glu-sensitive fluorescent gel was spin-coated onto the tip of an optical imaging fiber. The gel was prepared with L-Glu oxidase (GLOD), seminaphthofluorescein (SNAFL; a pH-sensitive fluorescent dye), and poly(acrylamide-co-*N*-acryloxysuccinimide) (PAN). Ammonia was liberated from the action of GLOD on L-Glu in the presence of O_2 and H_2O. Enhanced concentrations of ammonia decreased the fluorescence intensity of the dye (SNAFL). As the process is reversible and depends on the concentration of ammonia, L-Glu can be detected quantitatively. L-Glu was detected in the concentration range of 10 to 100 μM. The sensor was used to detect the action of L-Glu from the foregut plexus of *Manduca sexta* in the presence of the L-Glu re-uptake blocker dihydrokainate and the post-synaptic L-Glu receptor antagonist 6-cyano-7-nitroquinoxaline-2,3-dione (CNQX).

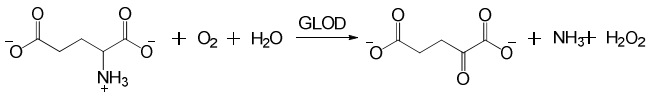

Fig. 33 Proposed mechanism of the action of GLOD with L-Glu.

Bonizzoni *et al.*[154] reported that a dicopper(II) octamine cage could serve as a selective receptor for L-Glu ions in water at pH 7 (Fig. 34). The rhodamine indicator (**23**) can then be captured by the dicopper (II) octamine cage, following in fluorescence quenching of the rhodamine dye. Displacement of the rhodamine indicator (**23**) from the cage by L-Glu restores the fluorescence of the dye completely. Fluorescence titration experiments revealed that the dimetallic cage **21** and the indicator **23** form a 1: 1 adduct with an association constant (K_{ass}) of 7.0 ± 0.2.

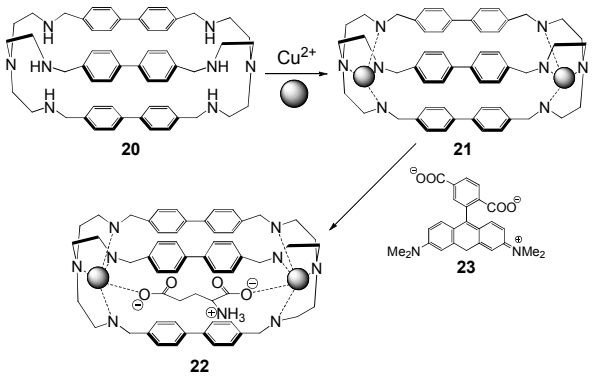

Fig. 34 Schematic representation for the mechanism for successive inclusion of 2 Cu^{2+} ions and a Glu within a bis-tren cage with diphenyl spacers.

Aspartate

Aspartic acid is a nonessential amino acid (α-amino acid). The conjugate base of aspartic acid is known as aspartate, which is a major excitatory neurotransmitter. It is present in high concentrations in the CNS and is released in a Ca^{2+}-dependent manner upon electrical stimulation *in vitro*. The normal concentration range of aspartate in CSF is 1.22±0.21μM[155-156]. It is involved in memory, learning, movement disorders, drug addiction, and other normal and abnormal physiological processes and behaviors.

A molecular ensemble for selective sensing of aspartate was reported by Anslyn *et al.*[157] (Fig. 35). Pyrocatechol violet **26** was used as the displacement unit because of its ability to chelate the Zn^{2+} in compounds **24** or **25**. A color change from yellow (λ_{max} = 445 nm) to a deep blue (λ_{max} = 647 nm) was observed in the presence of **24**-$(OAc)_2$ to a solution of the indicator in a 1:1 buffer/methanol co-solvent system (10 mM HEPES, pH 7.4). Binding constants of 3.75 × 10^5 and 6.0 × 10^4 M^{-1} for 1:1 binding of **24**:**26** and **25**:**26** were obtained, respectively. When various amino acids were added to the ensemble of **24**:**26** and **25**:**26** induced in a color change from deep blue to yellow. The binding constants of **25** with hydrophobic amino acids such as Gly, Val, and Phe were in the range of 1 × 10^4 M^{-1}.

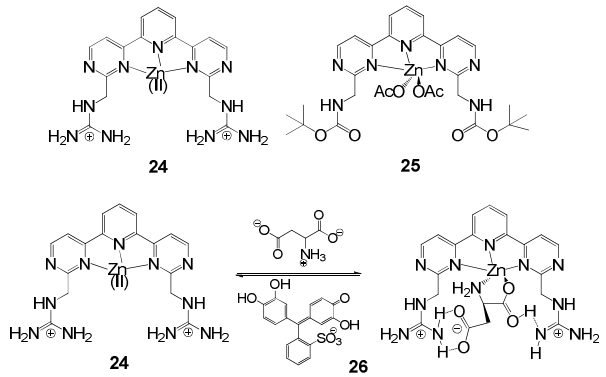

Fig. 35 Structures of **24**-**26** and proposed binding mode of **24** with amino acids.

Yong-Bing *et al.*[158] have synthesized 2 compounds, **27** and **28** (Fig. 36), which can recognize the enantiomers of *N*-acetyl-

aspartate over other amino acids. Both **27** and **28** have a calix[4]arene scaffold bearing dansyl fluorophore and (1*R*,2*R*)- or (1*S*,2*S*)-1,2-diphenylethylenediamine-binding sites. Absorption and fluorescence studies were carried out in dimethylsulfoxide. The fluorescence intensity was monitored at 532 nm following excitation at 344 nm. The fluorescence intensity was decreased upon addition of *N*-acetyl aspartate. Binding constants for *N*-acetyl D and L-aspartate were determined from fluorescence titration experiments. It was found that the ratio of the association constants for *N*-acetyl D and L-aspartate with **27** and **28** were 6.74 and 6.48, respectively.

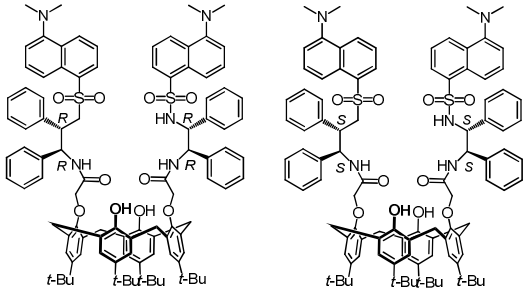

27 **28**

Fig. 36 Chemical structures of compound **27** and **28**.

γ-Aminobutyric Acid (GABA)

GABA is the major inhibitory neurotransmitter in the mammalian CNS. It is produced from L-glutamate by the catalytic reaction of the enzyme L-glutamic acid decarboxylase. GABA is released from electrically-stimulated inhibitory nerve cells. The normal level of GABA is in the range of 0.97±0.39μM.[155] Aberrant GABA regulation is implicated in sleep and eating disorders. The presence of low levels of GABA has also been linked to extreme anxiety.

A CE method in combination with laser-induced fluorescence (LIF) detection was employed for the quantification of GABA, glutamate (Glu), and aspartate (Asp) in *in vivo* microdialysis samples of cat brain.[159] In that study, synthetic cerebrospinal fluids were derivatized with FITC and the conditions for derivatization and separation were optimized. The separation of the samples was performed by CE and the analytes were quantified by LIF. The results were consistent with those obtained from HPLC.

Sensor **29** (Fig. 37) was used for selective detection of GABA zwitterions, over other ammonium ions, including glycine and its physiological precursor glutamic acid.[160] Sensor **29** was constructed with a backbone of fluorescent anthracene, with monoaza-18-crown-6 ether as a receptor for ammonium ions and a guanidinium ion as a receptor for carboxylate groups. The azacrown ether moiety can be involved in PET with anthracene. In presence of the GABA zwitterion, 70-fold enhancement of fluorescence at 424 nm was observed, with the excitation wavelength set at 372 nm. A methanol-water (3:2, v/v) mixture was used to allow host-guest binding via hydrogen bonding and ion pairing. To minimize the interference by protons, the experiments were carried out in basic conditions (pH 9.5).

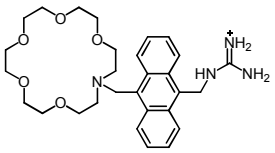

29

Fig. 37 Chemical structure of sensor **29**.

Glycine

Glycine is the simplest non-essential amino acid and it is synthesized in the body from serine, threonine, choline, hydroxyproline, and glyoxylic acid. It functions as an inhibitory neurotransmitter in the CNS. Glycine supports memory and mental functions in humans. The normal concentration range of glycine is 15.15±1.4μM.[155] Hyperglycinemia (elevated amounts of glycine) causes neonatal disease, lethargy, seizures, and mental retardation.

A quinoline-containing conjugated polymer can form a complex with Cu^{2+}. He et al [161] exploited this ensemble system as a platform for sensing amino acids (Fig. 38). When Cu^{2+} was added to a solution of **30**, the fluorescence intensity at 460 nm was quenched in THF. Upon addition of Gly, fluorescence recovery of **30** was observed, as Cu^{2+} was removed by the Gly from the **30**-Cu^{2+} complex. The detection limits of **30**-Cu^{2+} for Gly was calculated to be 7.7×10^{-9} M.

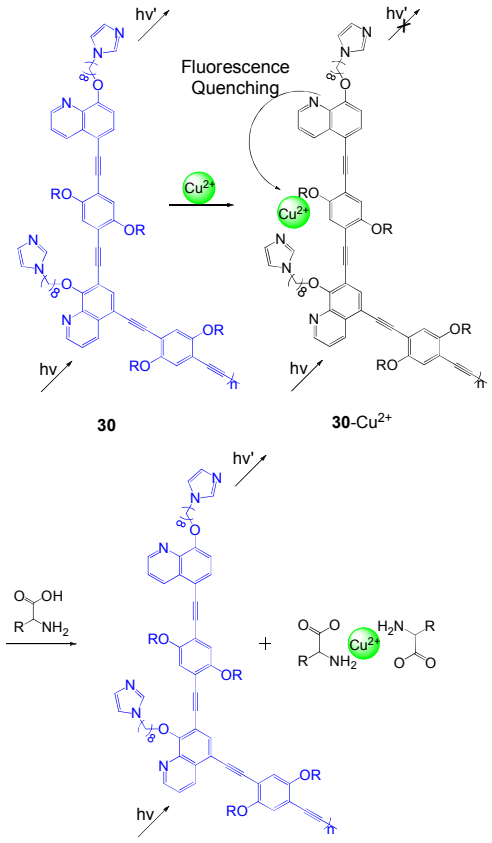

Fig. 38 Schematic representation of probe **30** for amino acids.

Durgadas *et al.*[162] reported a fluorescent gold nanocluster synthesized using bovine serum albumin (Au-BSA) for the detection of Cu^{2+} and Gly. Cu^{2+} can induce the fluorescence quenching of the Au-BSA, due to its capacity to bind to BSA. The emission peak of Au-BSA appeared at 645 nm and Cu^{2+} quenched the emission by 20%. Upon addition of Gly, Cu^{2+} was displaced from the surface of the Au-BSA and the quenched fluorescence could be retrieved. A good linear relationship between the enhancement of fluorescence and the concentration of Cu^{2+} in the range of 100 μM to 5 mM, with a detection limit of 50 μM, were observed.

An imidazole-functionalized di-substituted polyacetylene **31** was used as an α-amino acid chemosensor (Fig. 39).[163] It was shown that the quenched complex of **31** and Cu^{2+} could give respond quickly to glycine as well as other α-amino acids. Compound **31** was not selective for particular α-amino acids. The detection limit for glycine was 6.0×10^{-5} mol/L in aqueous solution.

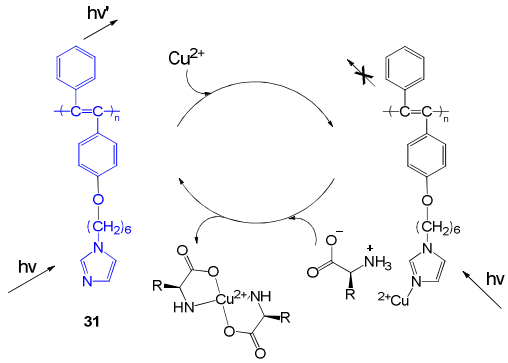

Fig. 39 The speculated conversion cycle of **31** in the presence of Cu^{2+} and α-amino acids.

Detection method of amines and unprotected amino acids by formation of highly fluorescent iminium ions was reported by Feuster and Glass[164] (Fig. 40). The interactions of the coumarin derivatives **32** and **33** with amino acids were examined using spectroscopic techniques under pH 7.4 buffer conditions (100 mM NaCl, 50 mM HEPES). When Glycine was added, the equilibrium formation of the fluorescent iminium ion was poor for **32** ($K_{eq} < 1$). In contrast, **33** sensitively sensed glycine, which then followed by formation of the iminium ion ($K_{eq} = 4.0$) to give a much larger (34 nm) red-shift in absorption. Results indicated that that the detection of all primary amines with sensor **33** was selective over secondary amines and hydroxy acids. Upon addition of Glycine, the enhancement of fluorescence intensity of **33** at 513 nm was ~26-fold.

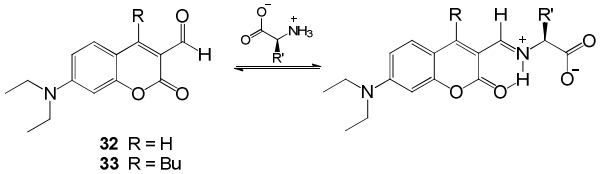

Fig. 40 The reaction mechanism of **32** and **33** with amino acids.

Tyrosine

Tyrosine is a nonessential amino acid that is synthesized in the body from another amino acid called phenylalanine. In the dopaminergic cells in the brain, L-tyrosine is converted to L-DOPA by the enzyme tyrosine hydroxylase. L-DOPA is the precursor to catecholamine neurotransmitters such as dopamine, epinephrine, and norepinephrine.[165] Low levels of tyrosine are involved with underactive thyroid, low blood pressure, and low body temperature. Deficiency of tyrosine may cause phenylketonuria, in which the body is unable to use the amino acid phenylalanine.

A label-free fluorescence method using functional magnetic NPs (MNPs) was adopted for quantitative detection of phosphorylated peptides/proteins in sample solutions by Chen *et al.*[166] (Fig. 41). The fluorescence molecule, riboflavin-5′-monophosphate (RFMP), was immobilized onto the surface of alumina-coated MNPs to generate the RFMP-Fe_3O_4@Al_2O_3 MNPs. The fluorescence of RFMP molecules was quenched while the molecules remained anchored on the surface of the MNPs. It was proposed that the addition of phosphorylated species, including *o*-phospho-L-tyrosine, induced displacement of the RFMP molecules from the RFMP-Fe_3O_4@Al_2O_3 MNPs with the assistance of microwave heating, which was followed by emission of fluorescence at 530 nm (λ_{ex} = 450 nm). The fluorescence intensities of **34** showed a good linear relationship regarding the concentration of the phosphopeptides in sample solutions, ranging from 10^{-8} to 5×10^{-7} M (R = 0.999). The phosphorylated species retained on the MNPs could also be directly characterized by MALDI-MS. The potential applications of this approach were discussed and the application for the rapid screening of the presence of phosphorylated fibrinopeptide A in serum samples collected from cancer patients was demonstrated.

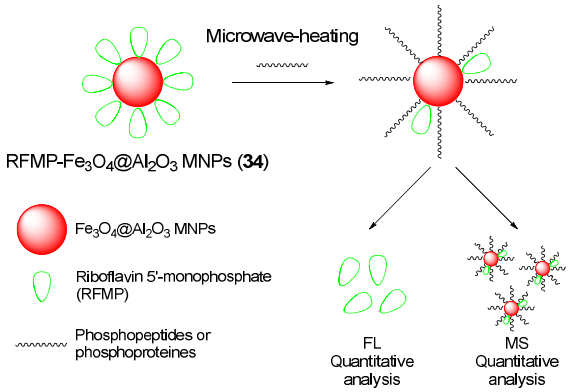

Fig. 41 Schematic representation of the quantitative and qualitative detection of phosphorylated peptides/proteins by fluorescence spectroscopy (FL) and MS.

Freeman *et al.*[167] prepared β-cyclodextrin (β-CD)-modified CdSe/ZnS QDs for sensing L-tyrosine using either a competitive FRET assay (Fig. 42) or direct electron transfer quenching. The emission of the CdSe/ZnS QDs overlaps the absorption of the rhodamine B incorporated in the β-CD. Upon excitation at 400 nm (excitation wavelength of QDs), emission of the rhodamine at 590 nm was observed, and the emission of CdSe/ZnS QDs at 535 nm was quenched. Upon addition of L-Tyr to the solution of **35**,

the emission intensity of rhodamine at 590 nm was gradually reduced with a subsequent increase in the emission band of the CdSe/ZnS QDs at 535 nm, because L-Tyr replaced rhodamine B from the cavities due to its strong affinity to β-CD. In comparison, the addition of D-tyrosine did not yield any significant signaling changes due to the low affinity of this enantiomer for β-CD. The association constants of L-tyrosine and D-tyrosine to β-CD were estimated to be 2.2×10^3 and 100 M^{-1}, respectively.

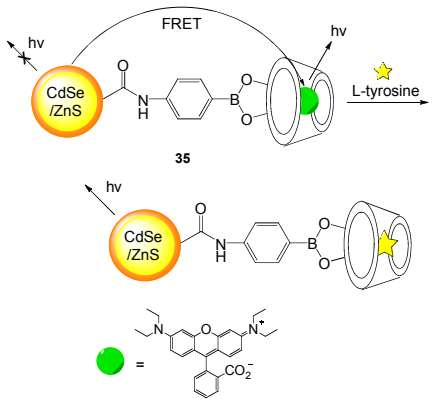

Fig. 42 Schematic representation of FRET assay used for sensing L-tyrosine with β-CD-modified CdSe/ZnS QDs (**35**) and receptor-bound rhodamine B.

Using the fluorophore dapoxyl and the macrocyclic host cucurbit[7]uril (CB7; composed of 7 glycoluril units), a multiparameter sensor array has been prepared by Bailey *et al.*[168] (Fig. 43). An indicator displacement strategy was employed according to the tandem assay principle described previously.[169-173] The method was based on the competition between the dapoxyl molecules and the products of Try, His, Arg, and Lys by decarboxylase for encapsulation into macrocyclics. Dapoxyl shows ~200-times stronger fluorescence intensity when it is complexed with CB7. The enzymatic decarboxylation of the amino acids converted the weak competitors (the amino acids) to strong competitors (more positively charged diamines), which led to consecutive displacement of the dapoxyl molecules from the complex. This resulted in quenching the dapoxyl fluorescence ('switched off' state) according to the amount of the converted amino acids. Although the method is limited for its low selectivity for specific amino acids, the selectivity can be enhanced by selecting decarboxylase enzymes specific for a particular analyte. The limiting sensitivity of this assay is ~2.4 nM per well in a microtiter plate format.

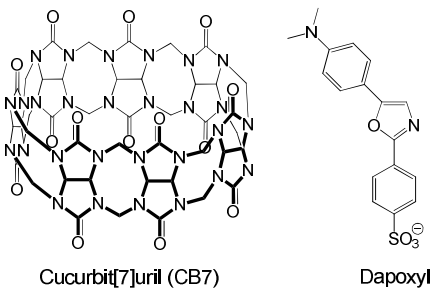

Fig. 43 Structures of cucurbit[7]uril and dapoxyl.

Ruta *et al.*[174] reported a sensitive aptamer-based assay for detecting target binding through a new fluorescence polarization (FP)-based strategy (Fig. 44). This method requires only a single fluorescent dye that can be attached at the end of aptamer, i.e., the method is very simple and less expensive. The method was based on the induced-fit binding system of nucleic acid aptamers. When L-tyrosinamide was added to an anti-L-tyrosinamide DNA aptamer-based system in Tris-HCl buffer (5 mM Tris-HCl, pH 7.5, 10 mM $MgCl_2$, 50 mM NaCl), the fluorescence anisotropy signal showed a significant increase due to the conformational change in DNA. This method was successfully applied to enantio-selective sensing of tyrosinamide and analysis of practical samples. The method was also able to detect L-argininamide.

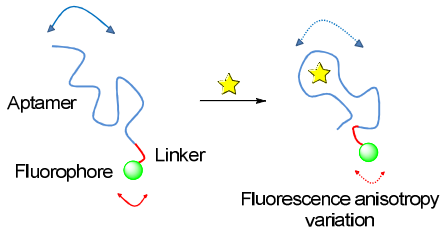

Fig. 44 Schematic representation of an aptasensor for a small molecule based on the non-competitive FP-based strategy. Double arrows indicate the possible local and global motions of the aptamer that contribute to the variation of the fluorescence anisotropy signal.

Tetsuya *et al.*[175] reported a fluorescent ribonucleopeptide (RNP) sensor specific for a phosphorylated tyrosine residues on protein surfaces (Fig. 45). The RNP receptors for sensing of specific phosphotyrosine residue were obtained from *in vitro* recognition of an RNA-derived pool of RNP. The phosphorylated tyrosine residue was within a defined amino-acid sequence, Gly-Tyr-Ser-Arg. A pool of fluorescent phosphotyrosine-binding RNPs was synthesized by combining the fluorophore-modified peptide and RNA subunits of phosphotyrosine-binding RNPs. A fluorescent RNP sensor was obtained for sequence-specific recognition of phosphorylated tyrosine through a screening process from a pool of fluorescent phosphotyrosine-binding RNPs. The sensor was able to discriminate phosphotyrosine against tyrosine, phosphoserine, and phosphothreonine. This sensor was successfully used for mapping phosphorylated-tyrosine-related signaling pathways in HeLa cell extracts.

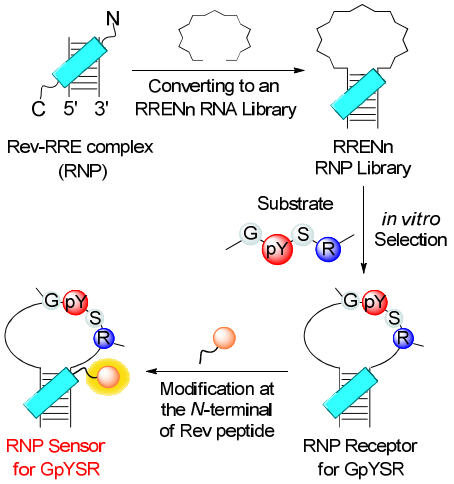

Fig. 45 Schematic representation for the strategy of getting RNP fluorescent sensors specific for a phosphotyrosine-containing peptide sequence, glycine-phosphotyrosine-serine-arginine (GpYSR). Combination of the RNA subunit of the GpYSR-binding RNP and a fluorophore-functionalized Rev peptide provided the GpYSR RNP fluorescent sensor. Rev stands for Regulator of Expression of Virion proteins.

3,3′-Dithiopropionic acid di(*N*-hydroxysuccinimide ester) (DPAN) can be used as a simple and robust monolayer adsorbate on the surface of gold NPs (AuNPs). *N*-hydroxisuccinimide (NHS) ester, which is an amine reactive cross-linker, is used for the bioconjugation of analytes onto the surface of AuNPs. Adsorption of DPAN on the surfaces of AuNPs induces aggregation, which changes the original red color of the AuNPs to blue (Fig. 46).[176] Upon addition of tyrosine into the aggregated state of AuNPs, the amine group of tyrosine was bioconjugated with the NPs through the NHS coupling unit in neutral or slightly basic conditions (pH: 7–8.5). As a result, aggregated AuNPs were dispersed, which caused color recovery from blue to red. This method can be utilized as a tool for predictive optical sensing for bioconjugation of amino acids. The sensor has no selectivity for tyrosine over other amino acids such as glycine, histidine, asparagine, glutamine, leucine, lysine, serine, and tryptophan. However, glycine, histidine, or tyrosine exhibit improved recovery behaviors over asparagine, glutamine, leucine, lysine, serine, and tyrosine under the optimun conditions used in the study.[176] The detection limit was as low as ~10^{-6} M in aqueous solutions.

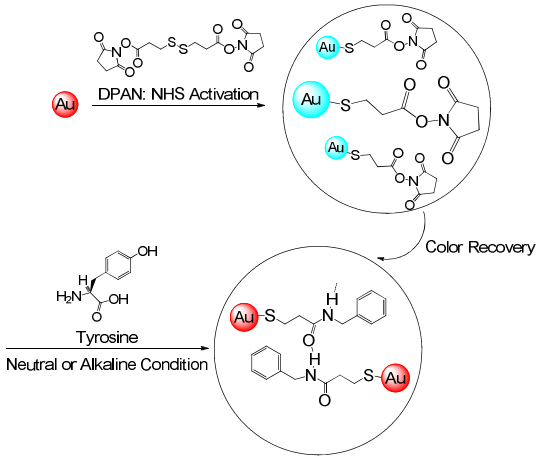

Fig. 46 Schematic representation of NHS coupling of tyrosine and 3,3'-dithiopropionic acid di(NHS ester) (DPAN) adsorbed on AuNPs.

Other Neurotransmitters

Adenosine

Adenosine is an inhibitory neurotransmitter that is associated with the regulation of CNS,[177] release of rennin,[178] and renal hemodynamics. Adenosine also plays important roles in sleep and arousal. Normal level of adenosine in human plasma is 180±40 nM.[179-180] Extracellular adenosine is important for controlling various cellular functions.[181-182] Quantitatve estimation of extracellular adenosine is necessary for the studies of cardiovascular and neurological conditions.

The low extracellular adenosine levels (ranging from undetectable levels to few mM)[183-185] and the interference from other nucleosides and adenine nucleotides are two complicating factors in the detection and quantification of adenosine. An electrochemical adenosine sensor is likely to have good sensitivity; such sensor has been commercialized and utilized in several studies for the measurement of adenosine concentrations in the CNS.[186] However, the electrochemical sensor requires three successive enzymatic reactions (catalyzed by adenosine deaminase, nucleoside phosphorylase, and xanthine oxidase). Adenosine aptamer sensors provide a more direct method to quantify adenosine concentrations, compared with the electrochemical sensor. Aptamers are functional oligonucleotides that can bind and display catalytic activity to pre-selected target (e.g. adenosine).[187-189]

Aptamers have high specificity and affinity to specific ligands. Adenosine aptamers conjugated with colored NPs, such as a malachite green aptamer, and G-quadruplex DNAzymes provided various signal readout methods.[190-193] ATP and AMP can not be distinguished by adenosine aptamer sensors because the aptamer is able to bind adenosine and adenine nucleotides equally well.[194-195] It is very difficult to quantify the extracellular adenosine concentrations lower than 1 μM because of the moderate binding affinity of the adenosine aptamer.

Lu and coworkers described a multiplex detection system for selective and sensitive determination of multiple analytes, including adenosine.[196] Two kinds of DNA-modified AuNPs (1

and 2), a DNA-midified QD (Q1), and a linker DNA involving the adenosine aptamer (colored green) (Fig. 47) were used to design the sensor. AuNP2 and Q1 were connected to the same DNA sequence. Two different conjugation chemistries (thiol DNA for AuNP2 and biotinylated DNA for streptavidin-coated Q1) were used to conjugate AuNP2 and Q1. Therefore, association between AuNP1 and AuNP2 or Q1 was observed through the same aptamer to self-assemble. AuNP2 was incorporated in the system to facilitate formation of large NP assemblies. The aggregation induced the quenching of fluorescence emission of the QD due to energy transfer to the neighboring AuNPs. The estimated ratio of AuNP1:AuNP2:Q1 was 3:3:1 in this study. Addition of adenosine switched the aptamer conformation into a complex structure. As a result, a number of base pairs was reduced to bind AuNP2 or Q1. The dissociation and disassembly of the nanostructure were occurred with a concomitant increase of luminescence intensity at 525. The increased luminescence intensity can be attributed to the increased distance between the QDs and AuNPs (quenchers). Higher concentrations of adenosine can induce intensity enhancement at faster rate. The quantification of adenosine was carried out to locate the emission intensity at 1 min after addition of adenosine. Concomitant with the enhancement of fluorescence, the color of AuNPs was changed from purple to red, and higher concentrations of adenosine induced a change to a more intense red coloration. The detection limit of this system for adenosine was 50 μM.

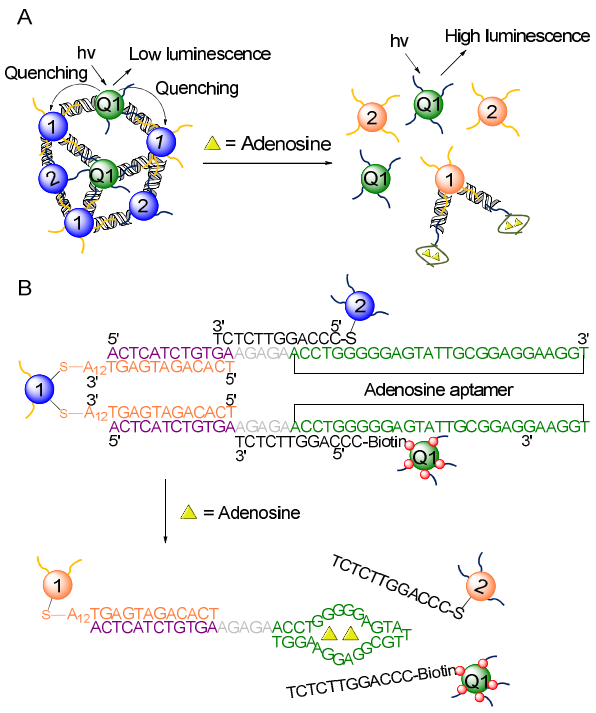

Fig. 47 (A) Schematic demonstration of the QD-encoded aptamer-linked nanostructures for adenosine sensing. (B) DNA sequences and NPs and modifications for the determination of adenosine are shown. 1, 2 are AuNPs and Q1 is the QD.

Urata *et al.*[197] prepared several single-stranded ATP-DNA aptamers that were placed with fluorophore as a donor and quencher as a donor on both ends of aptamers and studied the FRET-regulated fluorescent response due to the binding of adenosine. 6-Carboxyfluorescein (6-FAM) and *N*-[4-(4-dimethylamino)phenylazo]benzoic acid (DABCYL) were used as fluorophores (Fig. 48). **36** was expected that binding adenosine to the aptamers may stimulate the formation of base pairing of the stem region, which in turn might bring the 2 ends of the oligodeoxynucleotides (ODNs) closer to each other. In the presence of adenosine, the formation of base pairing of the stem region was stimulated in the aptamers, which then followed by the 2 ends of the oligodeoxynucleotides (ODNs) closer to each other. Consequently, fluorescence quenching occurs due to the FRET upon binding of adenosine. A linear relationship between the emission intensity and the level of adenosine was observed in the concentration range of 5–100 μM at 40°C. The detection of adenosine by this method was selective over cytidine, guanosine, uridine, and over nucleosides, excluding adenosine.

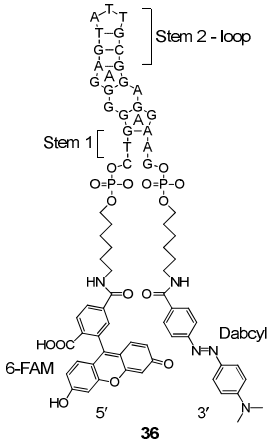

Fig. 48. Sequences and plausible secondary structure of fluorescent-labeled ATP aptamer. Binding site of adenine nucleotide in the aptamer is represented by 'A'.

An adenosine aptamer was engineered, consisting of two pieces of ssDNA, in which each piece could be attached with AuNPs through their 5′-thiol-modified ends.[198] In the presence of adenosine, two complementary pieces of aptamers attached with the NP reassemble into the intact aptamer tertiary structure, which leads to the formation of NP aggregates (Fig. 49). The adenosine functions as a molecular linker between the two pieces of ssDNA. Aggregation of NPs induced by different DNA structures can be distinguished through specific color changes by using surface plasmon resonance. Upon gradual addition of adenosine, the solution of AuNPs turns purple. The peak of the absorption spectra was at 520 nm and the detection limit of this colorimetric method was 0.25 mM for adenosine. The detection of adenosine was selective over uracil, guanine, and thiamine. The method was rapid, taking several minutes (less than half an hour) to complete. This method can be applied for the determination of many other small target analytes.

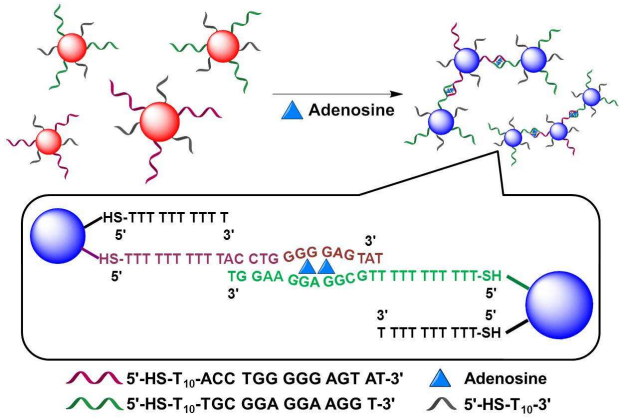

Fig. 49 Colorimetric detection of adenosine by target-induced assembly of AuNPs. The NPs were functionalized with two different DNA structures through thiol-AuNP chemistry. In presence of adenosine, the 2 kinds of NPs were attached by adenosine to form aggregates and the aggregation induced a color change from red to blue.

DNAzymes are catalytic DNAs. Aptamers are functional peptide that can bind and display catalytic activity to pre-selected targets. A spacer is an abasic site. A spacer was placed into duplex regions of an 8-17 DNAzyme to bind with a fluorophore, 2-amino-5,6,7-trimethyl-1,8-naphthyridine (ATMND).[199-200] The fluorescence emission was quenched after binding of the spacer with ATMND. In the presence of adenosine, structural changes were induced in the aptamer, which then followed by release of ATMND from the DNA duplex to give a marked fluorescence enhancement (Fig. 50), enabling detection of adenosine. In this method, the fluorescence intensity at 405 nm from the reaction of this sensor with adenosine was increased linearly in the range of 0–25 μM. The detection limit for adenosine was 3.4 μM.[201-203] This method was highly sensitive and selective for adenosine over 2 other nucleotides, uridine and cytidine, where little change regarding fluorescence was observed even with millimolar (mM) uridine or cytidine concentrations. The selectivity of this method for guanosine was not assessed due to a problem related to the solubility in aqueous solutions.

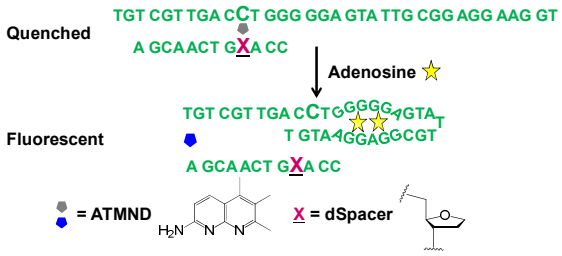

Fig. 50. Schematic representation of label-free fluorescent detection of adenosine.

AuNPs are used as an efficient sensing platform for the determination of various analytes due to their unique size-dependent surface plasmon resonance absorption.[204-206] Regarding target-induced switching of the aptamer structure, such as the aggregation of gold colloidal solution, a rapid and sensitive colorimetric platform for the detection of adenosine has been developed.[207]

AuNPs were wrapped with the random-coil aptamer under certain ionic strength conditions. The repulsive forces between NPs due to the negatively charged-aptamer (DNA) hindered aggregation of the NPs and the aptamer/AuNP solution remained well-dispersed. Contrary, adenosine can form target-aptamer complexes, disfavoring the adsorption of aptamer on the AuNP surface, which reduced the charge density on each AuNP. The reduced charge density in turn led to the aggregation of the Au colloidal solution (Fig. 51), following a color change from red to blue, a typical change for AuNP aggregation.[208] Thereby, this color change could be used to estimate the adenosine level in solution. Absorption peak of the AuNP/aptamer system (522 nm) was shifted to 540 nm and the peak intensity was reduced. A new broad absorption band (590–750 nm) was observed simultaneously. The absorbance ratio at 522 and 700 nm was calculated and used to estimate the degree of colloid aggregation, which served as an indicator, enabling colorimetric detection of adenosine. A linear relationship of the ratio of the absorbance at 522 to 700 nm with level of adenosine was applied in the range of 100 nM to 10 μM in the optimum conditions. The detection limit was 51.5 nM.

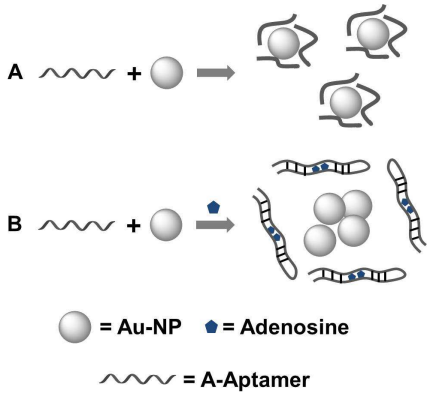

Fig. 51 Schematic illustration of a colorimetric probe for the detection of adenosine. System of the aptamer-target complex induces the aggregation of AuNPs, which leads to a color change from red to blue. In the scheme, A induces red coloration and B induces blue coloration.

A DNA aptamer specific for adenosine was used to discriminate between D- and L-adenosine.[209] There were three DNA segments in the adenosine sensor (Fig. 52); an aptamer with a nucleotide extension at the 5′-end (aptamer strand) capable of hybridizing to another DNA attached to a fluorophore (6-FAM) at its 5′-end (fluorophore strand), and the third DNA strand was modified with a quencher (DABCYL) at the 3′-end (quencher strand). In the absence of the target adenosine, the fluorescence emission from 6-FAM was suppressed by DABCYL through hybridization. In the presence of the target, the binding of the target by the aptamer disturbed the hybridization between the aptamer and quencher strands and resulted in release of the quencher strand, which in turn caused fluorescence enhancement. A 9-fold fluorescence enhancement occurred upon the addition of 1 mM D-adenosine into the DNA aptamers in 20 mM Tris-HCl buffer containing 300 mM NaCl and 5 mM $MgCl_2$ at pH 8.3. In contrast, 1 mM L-adenosine gave a fluorescence increase that was only one-third that induced by D-adenosine, indicating that the fluorescent adenosine sensor could be used to discriminate

between different optical isomers of adenosine. The relative dissociation constants were measured to be 0.7 mM for D-adenosine and 2.6 mM for L-adenosine.

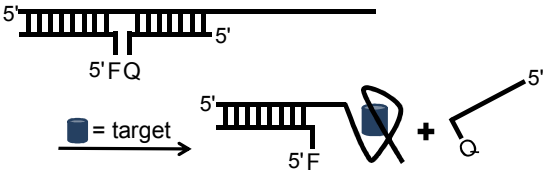

Fig. 52 Schematic illustration of the structure-switching method for DNA aptamers in the presence of a target (adenosine). F and Q represent the 6-FAM fluorophore and DABCYL quencher, respectively.

Chang *et al.*[178] demonstrated a label-free fluorescence analytical method for the determination of adenosine (Fig. 53). Their system comprised an adenosine-binding aptamer (Apt_{Ado}), platelet-derived growth factor (PDGF)-binding aptamer (Apt_{PDGF}), AuNPs, and the DNA-binding dye Oligreen (OG). Apt_{Ado} was used for the determination of adenosine and Apt_{PDGF} was used as a fluorescence signaling unit. The addition of adenosine induced a conformational switch of the Apt_{Ado} from a coiled to a G-quadruplex structure, which led to reduced binding of Apt_{Ado} onto the surface of AuNPs and yielded a change in the fluorescence of the aptamer-OG complexes. The addition of adenosine induced a structual change of the Apt_{Ado} from a coiled to a G-quadruplex conformation followed by reduced binding of Apt_{Ado} on the surface of AuNPs to yield a change in the fluorescence of the aptamer-OG complexes. The assay provided a limit of detection of 5.5 nM for adenosine in the presence of both Apt_{Ado}-modified AuNPs (Apt_{Ado}-AuNPs) and Apt_{PDGF}.

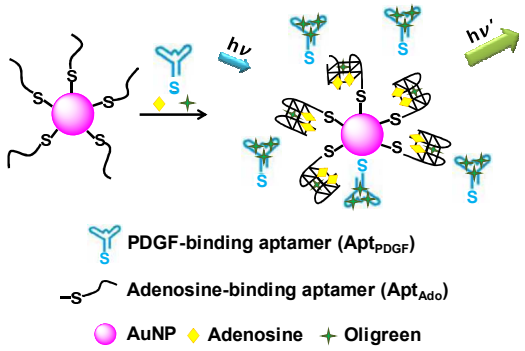

Fig. 53 Schematic demonstration of the label-free adenosine sensor based on the target-induced conformational change of aptamer. The sensor solution contains an adenosine-binding aptamer (Apt_{Ado}), Oligreen (OG), and AuNPs.

A catalytic and molecular beacon (CAMB) system has been prepared as a general platform for the sensitive determination of several analytes, including adenosine (Fig. 54).[210] A quencher was placed at the end of a DNAzyme strand and then hybridized with a fluorophore-labeled substrate strand. The substrate strand was structually transformed into a molecular beacon (MB) by extending both ends. Ten base pairs were inserted between the original DNAzyme substrate and the MB stem to increase conformational flexibility in the loop. In the presence of adenosine, the aptamer domain binds adenosine and forms a compact structure followed by hydrolysis the MB substrate, in the presence of Mg^{2+} as a cofactor, to release the fluorophore-labeled DNA strand, which generates an enhanced fluorescence signal within 20 minutes. On the other hand, the DNAzyme region of CAMB was unable to form an active structure to make a fluorescent fragment of the hairpin-structured substrate by catalytic reaction, even in the presence of Mg^{2+}. Likewise, the fluorescence enhancement rate increased according to the adenosine concentrations in a linear manner for the concentration range of 0–40 μM. The detection limit for adenosine was ~500 nM and the method was selective for adenosine over its analogue guanosine (500 μM).

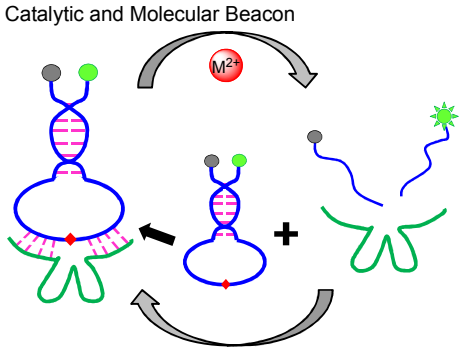

Fig. 54 Schematic representation of a CAMB sensor.

Nishizawa, Teramae and coworkers have used an abasic site-containing duplex DNA for the detection of adenosine (Fig. 55).[211] The fluorophore (ATMND) was attached in the abasic site of the duplex DNA aptamer, because of its strong affinity for the abasic site and its high fluorescence quantum yield. In the presence of adenosine, the fluorescence intensity of ATMND was enhanced due to the release of free ATMND from the abasic site of duplex DNA after binding of adenosine to the abasic site. In the presence of 150 mM adenosine, the emission intensity was enhanced 6.8-fold at 403 nm. A linear response was obtained in the concentration range of 5 to 100 μM and the detection limit was 2 μM. The detection was selective for adenosine over other nucleosides such as guanosine, cytidine, and thymidine. The detection was also very sensitive and was completed within a few minutes.

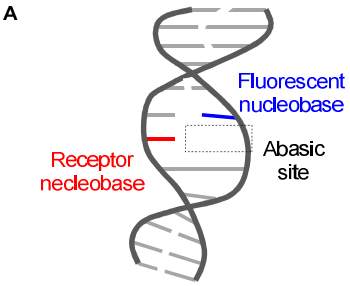

Fig. 55 (A) Schematic representation of a fluorescent signaling aptamer based on an abasic site-containing duplex DNA. (B) Names and sequences of duplex DNAs used in this study. P, X, and N indicate the 2-

AP (2-aminopurine), abasic site, and receptor base (G, C, A or T), respectively.

A triplex DNA aptamer was used for the selective and sensitive detection of adenosine.[177] The triplex DNA aptamer was prepared by a pair of furano-dU (dU indicates deoxyuridine) nucleotides in the binding site. Furano-dU is sensitive to the structural environment (Fig. 56). The pore of the triplex DNA aptamer was made in such a way that it can provide both Hoogsteen and Watson-Crick hydrogen bonding sites,[212] to allow strong interactions between the incoming adenosine and the neighboring 4 bases. The fluorescence intensity of this triplex DNA aptamer system was quenched by ~40% upon addition of adenosine. The Job plot indicated a 1:1 complex formation. The fluorescence response was linear in the concentration range of 50 to 400 nM adenosine and the detection limit was 50 nM. The triplex DNA aptamer was selective for adenosine over uridine, cytidine, guanosine, ATP, and AMP. This system worked much better than the duplex DNA aptamer systems.

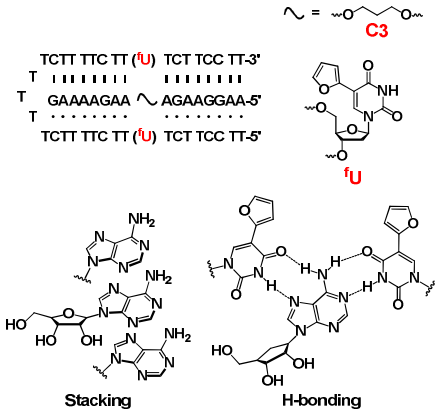

Fig. 56 Schematic presentation of the triplex DNA aptamer system and double clamping of adenosine by the surrounding bases of the aptamer.

Teramae *et al.*[213] used 3,5-diamino-6-chloro-2-pyrazine carbonitrile (DCPC) as the fluorescent reporter for binding to the abasic site-involving DNA duplexes by pseudo-base pairing (Fig. 57). The binding of adenosine to the aptamer induced tight pairing of the bases that flanked the abasic site. DCPC can be easily bound into the flanked abasic site of the stem. The binding of DCPC was associated with significant enhancement of fluorescence emission.

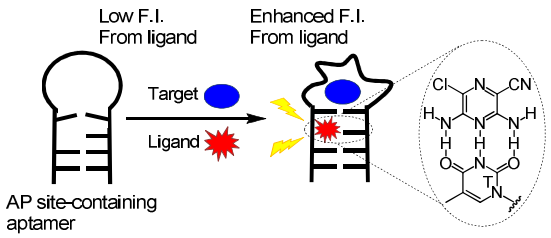

Fig. 57 Schematic illustration for fluorescence determination of adenosine (target) through the conformational change of an abasic site-containing aptamer in presence of abasic site-binding ligand (DCPC) and target. F.I. indicates fluorescence intensity.

DNA aptamers were fuctionalized on QDs, and QD/aptamer sensitively adsorbed on the sulface of AuNPs by electrostatic interaction between them followed by FRET to give an efficient fluorescence quenching (Fig. 58).[214] The presence of adenosine induced a conformational change in the DNA aptamers conjugated with QDs, which led them to be detached from the AuNPs. As a result, the fluorescence of the QDs was restored. The emission intensity was proportional with the adenosine concentration in this system.

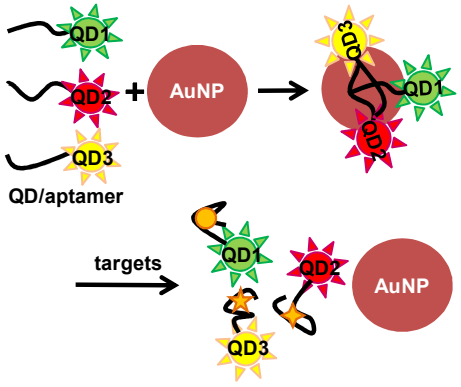

Fig. 58 Schematic representation for the fluorescence detection of adenosine (target) by unmodified AuNPs (umAuNP).

An FP-based method, based on an aptamer enzymatic cleavage protection method (Fig. 59), was applied for the detection of adenosine.[215] In this system, the size of the dye-labeled aptamer can be modulated by target-binding with the dye-labeled aptamer after enzymatic treatment. The fluorescent probe attached with the aptamer is an indicator of the size variation, due to the anisotropic signal change in fluorescence. On enzymatic treatment, labeled aptamers are cleaved into small DNA units, resulting in a lower fluorescence polarization signal. In the presence of the target adenosine, the conformation of the DNA aptamer is changed and the aptamers are protected somewhat from the enzymatic attack. The fluorescence polarization signal was increased due to the larger size of the aptamers. Phosphodiesterase I, which can cleave 5′-nucleotides from the 3′-end of DNA, was used as the catalytic enzyme.[216] Texas red (TR) and fluorescein were placed at the 5'-end of the DNA aptamers. Using a TR-labeled probe, the detection limit for adenosine was estimated to be 25 μM. This method was selective for adenosine over inosine and guanosine.

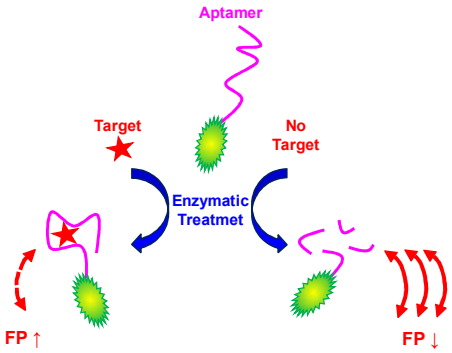

Fig. 59 Schematic illustration of FP-based sensing of adenosine (target), based on target-mediated protection of the aptamer from phosphodiesterase I-induced cleavage.

In a similar adenosine assay system,[217] adenosine protected the DNA aptamer from enzymatic cleavage after binding with the DNA aptamer. In the absence of adenosine, the aptamer sensitively sensed the phosphodiesterase I enzymatic probe followed by enzymatic cleavage to give the release of mononucleotides and short DNA fragments (Fig. 60).[217] The short DNA fragments stabilized the AuNPs upon addition of salt through favorable electrostatic interactions and the particles were dispersed in the solution, due to which the color of the solution appeared red. In the presence of adenosine, when the DNA aptamers were protected from the enzymatic attack, long DNA molecules upon addition of salt were unable to provide electrostatic stabilization to the AuNPs. As a result, the NPs were aggregated and the solution color turned to blue. The target molecules were quantitatively estimated by monitoring the ratio of absorbances at 650 and 520 nm. The adenosine assay displayed a linear response between 0–100 μM and the detection limit was 1 μM adenosine. This assay was selective for adenosine over inosine.

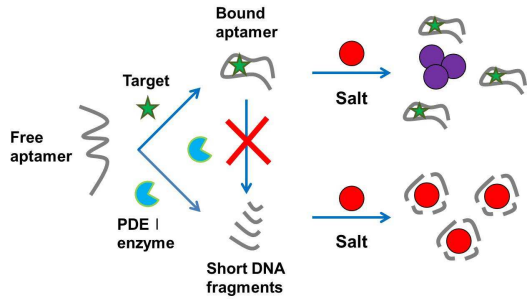

Fig. 60 Schematic illustration of aptamer assay based on enzymatic cleavage protection.The unmodified AuNPs were used as colorimetric reporters for the detection of adenosine. PDEI: phosphodiesterase I enzyme.

Lu *et al.*[218] combined the 2 methods, catalytic and molecular beacon (CAMB) and label-free fluorescent sensors, using an abasic site to develop a new label-free CAMB sensor that possessed the advantages of both methods for the efficient detection of adenosine (Fig. 61). The detection limit of adenosine using the combination method was 1.4 μM, with good selectivity over other nucleosides.

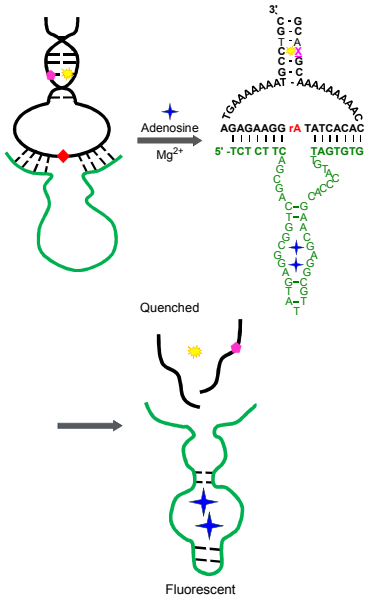

Fig. 61 Schematic illustration of fluorescent detection of adenosine by the label-free CAMB sensor with an abasic site.

Conclusions and Future Perspectives

In this review, we summarize substantial progresses in the fluorescence-based neurotransmitter sensing over the last twelve years (from 2000 to 2012), considering the sensing mechanism, the compatibility with biological samples, and the applications to biological imaging. Indeed, it is evident that the fluorescence-based methods have some advantages over other analytical methods, such as simple procedures, fast analysis times, cheap instrumentation, and high sensitivity. Yet, further improvement in the fluorophore design seems to be nessessary since only a few publications were successful to demonstrate its application to the intact biological samples (e.g., cerebrospinal fluids) and little to the live cells. To overcome these apparent limitations in the applications of the fluorescence-based neurotransmitter sensing to the intact biological systems, the fluorescence sensors should be improved in many aspects such as the water solubility, cell permeability, photostability, and selectivity to a specific neurotransmitter. Also, the longer-wavelength probes (near infrared) would be recommended for application to the live cell or tissue imaging of neurotransmitters. Further studies in CSF, plasma, serum, blood platelet and urine of patients with different neurological diseases are required for clinical diagnostics. Such simple and inexpensive methods are very urgent for routine analysis purpose. Better understanding of the sensing mechanism along with rich information on brain structure and function will accelerate development of the advanced neurotransmitter sensors in the near future.

Acknowledgment

This work was supported by the CRI project (2009-0081566) (JSK) and by the Basic Science Research Program (NRF-2012R1A1A2006259) of the National Research Foundation of Korea funded by the Ministry of Education, Science, and Technology.

List of Abbreviations

Ach	acetylcholine
AMP	adenosine monophosphate
ATP	adenosine triphosphate
ATMND	2-amino-5,6,7-trimethyl-1,8-naphthyridine
BSA	bovine serum albumin
CAMB	catalytic and molecular beacon
CB[8]	cucurbit[8]uril
CD	cyclodextrin
CE	capillary electrophoresis
CE-LIF	capillary electrophoresis-laser-induced fluorescence
CNS	central nervous system
CNQX	6-cyano-7-nitroquinoxaline-2,3-dione
CP-MAS	^{13}C cross polarization-magic angle spinning
DABCYL	*N*-[4-(4-dimethylamino)phenylazo]benzoic acid
DCPC	3,5-diamino-6-chloro-2-pyrazine carbonitrile
DFT	density functional theory
DNA	Deoxyribonucleic acid
DOPA	3,4-Dihydroxyphenylalanine
DPE	1,2-diphenylethylenediamine
DPAN	3,3′-Dithiopropionic acid di(*N*-hydroxysuccinimide ester)
DPT^{2+}	2,7-dimethyldiazaphenanthrenium
6-FAM	6-Carboxyfluorescein
FITC	fluorescein-5-isothiocyanate
FP	fluorescence polarization
FRET	florescence resonance energy transfer
GABA	γ-aminobutyric acid
GO	Graphene oxide
HEPES	2-[4-(2-hydroxyethyl)piperazin-1-yl]ethanesulfonic acid
HPLC	high performance liquid chromatography
5-HT	5-hydroxytryptamine (serotonin)
LC	liquid chromatography
MALDI-MS	Matrix-assisted laser desorption/ionization mass spectrometry
MCE	microchip electrophoresis
MCM	Mobil Crystalline Materials
Me_2DAP^{2+}	2,7-dimethyldiazapyrenium dication
MLCT	metal-to-ligand charge transfer
MSN	mesoporous silica nanosphere
MOPS	3-(N-morpholino)propanesulfonic acid
NMR	nuclear magnetic resonance
NHS	*N*-hydroxisuccinimide
NPs	nanoparticles
ODHMIQ	6-oxo-4,7-dihydroxy-2-methyl-*iso*-quinoline
ODNs	oligodeoxynucleotides
ODS	octadecylsilane
OG	Oligreen
OPTA	*o*-phthalic hemithioacetal
OPA	*o*-phthalaldehyde
PAN	poly(acrylamide-co-*N*-acryloxysuccinimide
PDA	polydiacetylene
PDGF	platelet-derived growth factor
PET	photo-induced electron transfer
PLA	poly-(lactic acid)
PPE	Poly(*p*-phenylene ethynylene)
PSE	4-(1-pyrene)butyric acid *N*-hydroxysuccinimide ester
P-TiO_2	phosphate-modified titanium dioxide
QDs	quantum dots
RFMP	riboflavin-5′-monophosphate
RNA	ribonucleic acid
RNP	fluorescent ribonucleopeptide
RSD	relative standard deviation
SBA	Santa Barbara Amorphous
SDS	sodium dodecyl sulfate
SNAFL	seminaphthofluorescein
TR	Texas red
Tris-HCl	tris(hydroxymethyl)aminomethane hydrochloride

Notes and References

1. E. R. Kandel, J. H. Schwartz, T. M. Jessell, S. A. Siegelbaum and A. J. Hudspeth, *Principles of Neural Science*, *5th ed.*, McGraw-Hill, New York, 2012.
2. R. A. Webster, *Neurostransmitters, drugs and brain function*, John Wiley & Sons, New York, 2001.
3. O. Loewi, *Pflüg. Arch. Eur. J. Phy*., 1921, **189**, 239.
4. D. S. Goldstein, G. Eisenhofer and R. McCarty, *Catecholamines: Bridging Basic Science with Clinical Medicine*, Academic Press, San Diego, 1998.
5. A. P. de Silva, H. Q. N. Gunaratne, T. Gunnlaugsson, A. J. M. Huxley, C. P. McCoy, J. T. Rademacher and T. E. Rice, *Chem. Rev*., 1997, **97**, 1515.
6. X. Chen, X. Tian, I. Shin, and J. Yoon, *Chem. Soc. Rev.*, 2011, **40**, 4783.
7. A. W. Czarnik, *Fluorescent Chemosensors for Ion and Molecule Recognition*, American Chemical Society, Washington, DC, 1992.
8. J. R. Lakowicz, *Principles of Fluorescence Spectroscopy*, Plenum Press, New York, 1983.
9. J. R. Lakowicz, *Fluorescence Spectroscopy of Biomolecules. In Encyclopedia of Molecular Biology and Molecular Medicine*, R. A. Meyers, Ed., VCH Publishers, New York, 1995.
10. H. Szmacinski, I. Gryczynski and J. R. Lakowicz, *Photochem. Photobiol.*, 1993, **58**, 341.
11. T. Yanagida and Y. Ishii, *Single Molecule Dynamics in Life Science*, Wiley-VCH: Weinheim, Germany, 2009.
12. S. H. Lee, J. Y. Kim, J. Ko, J. Y. Lee and J. S. Kim, *J. Org. Chem.*, 2004, **69**, 2902.
13. Y. H. Lee, M. H. Lee, J. F. Zhang and J. S. Kim, *J. Org. Chem.*, 2010, **75**, 7159.
14. H. J. Kim and J. S. Kim, *Tetrahedron Lett.*, 2006, **47**, 7051.
15. J. S. Kim, H. J. Kim, H. M. Kim, S. H. Kim, J. W. Lee, S. K. Kim and B. R. Cho, *J. Org. Chem.*, 2006, **71**, 8016.
16. K. C. Ko, J.-S. Wu, H. J. Kim, P. S. Kwon, J. W. Kim, R. A. Bartsch, J. Y. Lee and J. S. Kim, *Chem. Commun.*, 2011, **47**, 3165.
17. I. V. Korendovych, R. A. Roesner and E. V. Rybak-Akimova, *Adv. Inorg. Chem.*, 2007, **59**, 109.
18. C. A. Piantadosi, *Free Rad. Bio. & Med.*, 2008, **45**, 562.

19. T. B. Settersten, *Preprints of Symposia - Am. Chem. Soc., Div. of Fuel Chem.*, 2007, **52**, 52.
20. G. I. Likhtenshtein, *Appl. Biochem. Biotech.*, 2009, **152**, 135.
21. X. Ye, S. S. Rubakhin and J. V. Sweedler, *Analyst*, 2008, **133**, 423.
22. A. Gomes, E. Fernandes and J. L. F. C. Lima, *J. Fluoresc.*, 2006, **16**, 119.
23. S. A. Hilderbrand, M. H. Lim and S. J. Lippard, *Top. Fluoresc. Spec*., 2005, **9**, 163.
24. N. Sekar, *Colourage*, 2001, **48**, 50.
25. B. Kalyanaraman, *Biochem. Soc. Trans.*, 2011, **39**, 1221.
26. N. Soh, *Anal. Bioanal. Chem.*, 2006, **386**, 532.
27. V. S. Lin and C. J. Chang, *Curr. Opin. Chem. Biol.*, 2012, **16**, 595.
28. N. Kumar, V. Bhalla and M. Kumar, *Coord. Chem Rev.*, 2013, **257**, 2335.
29. J. Lee, S. Lee, K. Ragunathan, C. Joo, T. Ha and S. Hohng, *Angew. Chem. Int. Ed.*, 2010, **49**, 9922.
30. K. Kubo, *Top. Fluoresc. Spectrosc.*, 2005, **9**, 219.
31. G. J. Kavarnos, *Fundamentals of Photoinduced Electron Transfer*, VCH Publishers, New York, 1993.
32. H. S. Jung, J. H. Han, T. Pradhan, S. Kim, S. W. Lee, J. L. Sessler, T. W. Kim, C. Kang and J. S. Kim, *Biomaterials*, 2012**, 33**, 945.
33. H. S. Jung, T. Pradhan, J. Han, K. J. Heo, C. Kang and J. S. Kim, *Biomaterials*, 2012**, 33**, 8495.
34. J. F. Zhang, S. Kim, J. H. Han, S. J. Lee, T. Pradhan, Q. Y. Cao, S. J. Lee, C. Kang and J. S. Kim, *Org. Lett.*, 2011, **13**, 5294.
35. W. Baumann and Z. Nagy, *Pure & Appl. Chem.*, 1993*,* **65**, 1729.
36. F. M. Winnik, *Chem. Rev.*, 1993, **93**, 587.
37. L. G. Kostrikis, S. Tyagi, M. M. Mhlanga, D. D. Ho and F. R. Kramer, *Science*, 1998, **279**, 1228 and references therein.
38. R. Nutiu and Y. Li, *J. Am. Chem. Soc.*, 2003, **125**, 4771.
39. Z. Zhu, C. Ravelet, S. Perrier, V. Guieu, B. Roy, C. Perigaud and E. Peyrin, *Anal. Chem.*, 2010, **28**, 4613.
40. A. W. Czarnik, *Fluorescent Chemosensors for Ion and Molecule Recognition*, ACS: Washington, DC, 1992.
41. M.-Y. Chae and A. W. Czarnik, *J. Am. Chem. Soc.*, 1992, **114**, 9704.
42. Y.-K. Yang, K.-J. Yook and J. Tae, *J. Am. Chem. Soc.*, 2005, **127**, 16760.
43. F. Song, S. Watanabe, P. E. Floreancig and K. Koide, *J. Am. Chem. Soc.*, 2008, **130**, 16460.
44. V. Dujols, F. Ford and A. W. Czarnik, *J. Am. Chem. Soc.*, 1997, **119**, 7386.
45. J. P. Desvergne and A. W. Czarnik, *Chemosensors for Ion and Molecule Recognition*; *NATO Asi Series, Series C*, Kluwer Academic Publishers, London, 1997.
46. T. Nagatsu and H. Ichinose, *Cell. Mol. Neurobiol.*, 1999, **19**, 57.
47. T. Suominen, P. Uutela, R. A. Ketola, J. Bergquist, L. Hillered, M. Finel, H. Zhang, A. Laakso, R. Kostiainen*, PLOS one*, 2013, **8**, e68007.
48. P. Sótonyi, B. Merkely, M. Hubay, J. Járay, E. Zima, P. Soós, A. Kovács and I. Szentmáriay, *Toxicol. Sci.*, 2004, **77**, 368.
49. J. L. Neumeyer and R. G. Booth, *In Principles of Medicinal Chemistry*, *4th ed. Chapter 13*, W. O. Foye, T. L. Lemke and D. A. Williams, Eds., Lea and Febiger, Philadelphia, 1995.
50. E. L. Bravo and R. C. Tarazi, *N. Engl. J. Med.*, 1979, **301**, 682.
51. S. Kolusheva, O. Molt, M. Herm, T. Schrader and R. Jelinek, *J. Am. Chem. Soc.*, 2005, **127**, 10000.
52. S. S. Jr. Simons and D. F. Johnson, *Anal. Biochem.*, 1978, **90**, 705.
53. S. S. Jr. Simons and D. F. Johnson, *J. Org. Chem.*, 1978, **43**, 2886.
54. F. Dai, V. P. Burkert, H. N. Singh and W. L. Hinze, *Microchem. J.*, 1997, **57**, 166.
55. V. S.-Y. Lin, C.-Y. Lai, J. Huang, S.-A. Song and S. Xu, *J. Am. Chem. Soc.*, 2001, **123**, 11510.
56. F. M. Raymo and M. A. Cejas, *Org. Lett.*, 2002, **4**, 3183.
57. D. R. Radu, C.-Y. Lai, J. W. Wiench, M. Pruski and V. S.-Y. Lin, *J. Am. Chem. Soc.*, 2004, **126**, 1640.
58. S. A. Gomez-Lopera, R. C. Plaza and A. V. Delgado, *J. Colloid Interface Sci.*, 2001, **240**, 40.
59. A. Coskun and E. U. Akkaya, *Org. Lett.*, 2004, **6**, 3107.
60. K. E. Secor and T. E. Glass, *Org. Lett.*, 2004, **6**, 3727.
61. R. Jelinek and S. Kolusheva, *Biotechnol. Adv.*, 2001, **19**, 109.
62. S. Kolusheva, T. Shahal and R. Jelinek, *J. Am. Chem. Soc.*, 2000, **122**, 776.
63. S. Kolusheva, E. Wachtel and R. Jelinek, *J. Lipid Res.*, 2003, **44**, 65.
64. Z. Orynbayeva, S. Kolusheva, E. Livneh, A. Lichtenshtein, I. Nathan and R. Jelinek, *Angew. Chem., Int. Ed.*, 2005, **44**, 1092.
65. M. Herm, O. Molt and T. Schrader, *Chem. Eur. J.*, 2002, **8**, 1485.
66. M. Ackenheil, M. Frohler, G. Goldig, G. Rall and D. Welter, *Arzneimittelforsch/Drug Res.*, 1982, **32**, 893.
67. C. Holmes, G. Eisenhofer and D. S. Goldstein, *J. Chromatogr. Biomed. Appl.*, 1994, **653**, 131.
68. M. Maue and T. Schrader, *Angew. Chem., Int. Ed.*, 2005, **44**, 2265.
69. M. A. Cejas and F. M. Raymo, *Langmuir*, 2005, **21**, 5795.
70. V. Sindelar, M. A. Cejas, F. A. Raymo, W. Chen, S. E. Parker and A. E. Kaifer, *Chem. Eur. J.*, 2005, **11**, 7054.
71. R. Ballardini, V. Balzani, A. Credi, M. T. Gandolfi, S. J. Langford, S. Menzer, L. Prodi, J. F. Stoddart, M. Venturi and D. J. Williams, *Angew. Chem. Int. Ed. Engl.*, 1996, **35**, 978.
72. Y. Kim, J. Whitten and T. M. Swager, *J. Am. Chem. Soc.*, 2005, **127**, 12122.
73. Y. Kim and T. M. Swager, *Macromolecules*, 2006, **39**, 5177.
74. H.-P. Wu, T.-L. Cheng and W.-L. Tseng, *Langmuir*, 2007, **23**, 7880.
75. R. Freeman, L. Bahshi, T. Finder, R. Gill and I. Willner, *Chem. Commun.*, 2009, **7**, 764.
76. D. A. Dikin, S. Stankovich, E. J. Zimney, R. D. Piner, G. H. B. Dommett, G. Evmenenko, S. T. Nguyen and R. S. Ruoff, *Nature*, 2007, **448**, 457.
77. J. I. Paredes, S. Villar-Rodil, A. Martinez-Alonso and J. M. D. Tascon, *Langmuir*, 2008, **24**, 10560.
78. Z. Liu, J. T. Robinson, X. Sun and H. Dai, *J. Am. Chem. Soc.*, 2008, **130**, 10876.
79. N. Mohanty and V. Berry, *Nano Lett.*, 2008, **8**, 4469.
80. M. Zhou, Y. M. Zhai and S. J. Dong, *Anal. Chem.*, 2009, **81**, 5603.
81. Y. Xu, Z. Liu, X. Zhang, Y. Wang, J. Tian, Y. Huang, Y. Ma, X. Zhang and Y. Chen, *Adv. Mater.*, 2009, **21**, 1275.
82. R. S. Swathi and K. L. Sebastian, *J. Chem. Phys.*, 2008, **129**, 054703.
83. R. S. Swathi and K. L. Sebastian, *J. Chem. Phys.*, 2009, **130**, 086101.
84. J.-L. Chen, X.-P. Yan, K. Meng and S.-F. Wang, *Anal. Chem.*, 2011, **83**, 8787.
85. M. J. Koenigbauer, S. P. Assenza, R. C. Willoughby and M. A. Curtis, *J. Chromatogr. Biomed. Appl.*, 1987, **413**, 161.
86. E. Kojima, M. Kai and Y. Ohkura, *J. Chromatogr.*, 1993, **612**, 187.
87. A. M. Krstulovic and A. M. Powell, *J. Chromatogr.*, 1979, **17**, 345.
88. Y. Y. Su, J. Wang and G. N. Chen, *Talanta*, 2005, **65**, 531.
89. M. M. Karim, S. M. Alam and S. H. Lee, *J. Fluoresc.*, 2007, **17**, 427.
90. X. Wu, C. L. Tong, B. Y. Su, F. Huang and J. H. Yang, *J. Shandong Univ. China*, 1998, **34**, 352.
91. C. L. Tong, G. C. Lu and Z. L. Xu, *J. Zhejang Univ. Sci. Ed.*, 2000, **27**, 530.
92. Y. Guo, J. Yang, X. Wu and A. Du, *J. Fluoresc.*, 2005, **15**, 131.
93. J. Yang, G. Zhou, N. Jie, R. Han, C. Lin and J. Hu, *Microchem. J.*, 1996, **54**, 41.
94. Y. Guo, J. Yang, X. Wu and H. Mao, *Talanta*, 2007, **73**, 227.
95. W. K. Adeniyi and A. R. Wright, *Spectrochim. Acta, Part A*, 2009, **74A**, 1001.
96. H. Jeong, H. Kim and S. Jeon, *Microchem. J.*, 2004, **78**, 181.
97. T. Yoshitake, K. Fujino, J. Kehr, J. Ishida, H. Nohta and M. Yamaguchi, *Anal. Biochem*., 2003, **312**, 125.
98. Z. D. Peterson, D. C. Collins, C. R. Bowerbank, M. L. Lee and S. W. Graves, *J. Chromatogr. B*, 2002, **776**, 221.
99. M. A. Fotopoulou and P. C. Ioannou, *Anal. Chim. Acta*, 2002, **462**, 179.
100. D. L. Kuhlenbeck, T. P. O'Neill, C. E. Mack, S. H. Hoke and K. R. Wehmeyer, *J. Chromatogr. B*, 2000, **738**, 319.
101. P. Cañizares and M. D. Luque de Castro, *Anal. Chim. Acta*, 1995, **317**, 335.
102. M. H. Sorouraddin, J. L. Manzoori, E. Kargarzadeh and A. M. Shabani, *J. Pharm. Biomed. Anal.*, 1998, **18**, 877.
103. M. Yoshitake, H. Nohta, H. Yoshida, T. Yoshitake, K. Todoroki and M. Yamaguchi, *Anal. Chem*., 2006, **78**, 920.

104.M. M. Karim, S. M. Alam and S. H. Lee, *J. Fluoresc.*, 2007, **17**, 427.
105.C. Firk and C. R. Markus, *J. Psychopharm.*, 2007, **21**, 538.
106.E. Pobozy, A. Michalski, J. Sotowska-Brochocka and M. Trojanowicz, *J. Sep. Sci.*, 2005, **28**, 2165.
107.F. Artigas, M. J. Sarrias, E. Martinez, E. Gelpi, *Life Sciences*, 1985, **37**, 441.
108.A. Chattopadhyay, R. Rukmini and S. Mukherjee, *Biophys. J.*, 1996, **71**, 1952.
109.S. Umeda, G. W. Stagliano, M. R. Borenstein and R. B. Raffa, *J. Pharmacolog. Toxicolog. Meth.*, 2005, **51**, 73.
110.S. Ohla, P. Schulze, S. Fritzsche and D. Belder, *Anal. Bioanal. Chem.*, 2011, **399**, 1853.
111.P. Schulze, M. Schuettpelz, M. Sauer and D. Belder, *Lab Chip*, 2007, **7**, 1841.
112.Y. Takashi, F. Kaoru, K. Jan, I. Junichi, N. Hitoshi and Y. Masatoshi, *Anal. Biochem.*, 2003, **312**, 125.
113.M. Kai, H. Iida, H. Nohta, M. K. Lee and K. Ohta, *J. Chromatogr. B*, 1998, **720**, 25.
114.P. Qian and J. Chongqiu, *J. Fluoresc.*, 2007, **17**, 339.
115.U. Sidney, W. Herbert, T. C. Carroll, *J. Biol. Chem.*, 1954,337.
116.R. D. Arraez, C. A. Antonio Segura, B. C. Cruces and G. A. Fernandez, *Biomed. Chromatogr.*, 2004, **18**, 422.
117.Y. Hideyuki, K. Fumito, Y. Makoto, T. Kenichiro, N. Hitoshi and Y. Masatoshi, *Anal. Sci.*, 2007, **23**, 485.
118.Y. Makoto, N. Hitoshi, Y. Hideyuki, Y. Takashi, T. Kenichiro and Y. Masatoshi, *Anal. Chem.*, 2006, **78**, 920.
119.S. Kim, T. Sakano, A. Tanaka and T. Nagamura, *Mol. Cryst. Liq. Cryst.*, 2011, **538**, 304.
120.A. G. Bracamonte and A. V. Veglia, *Talanta*, 2011, **83**, 1006.
121.J. K. Khandelwal , L. B. Hough , J. P. Green , *Klinische Wochenschrift ,* 1983, **60**, 914.
122.U. Kallweit, K. Aritake, C. L Bassetti, S. Blumenthal, O. Hayaishi, M. Linnebank, C. R Baumann, Y. Urade *Fluids and Barriers of the CNS* 2013, **10**, 19.
123.Y. Ling, W. Wang and A. E. Kaifer, *Chem. Commun.*, 2007, **6**, 610.
124.T. Yoshitake, F. Ichinose, H. Yoshida, K-i Todoroki, J. Kehr, O. Inoue, H. Nohta and M. Yamaguchi, *Biomed. Chromatogr*., 2003, **17**, 509.
125.D. Seto, N. Soh, K. Nakano and T. Imato, *Anal. Biochem.*, 2010, **404**, 135.
126.D. Seto, N. Soh, K. Nakano and T. Imato, *Bioorg. Med. Chemi. Lett.*, 2010, **20**, 6708.
127.C.-F. Chow, H.-K. Kong, S.-W. Leung, B. K. W. Chiu, C.-K. Koo, E. N. Y. Lei, M. H. W. Lam, W.-T. Wong and W.-Y. Wong, *Anal. Chem.*, 2011, **83**, 289.
128.T. Tsai, *J. Chromatogr. B*, 2000, **747**, 111.
129.L. Doretti, D. Ferrara, S. Lora, F. Schiavon and F. M. Veronese, *Enzyme Microb. Technol.*, 2000, **27**, 279.
130.J. Marty, K. Sode and I. Karube, *Anal. Chim. Acta*, 1989, **228**, 49.
131.T. Yao, *Anal. Chim. Acta*, 1983, **153**, 169.
132.J. D. Salamone and D.B. Neill, *Anal. Chim. Acta*, 1983, **146**, 149.
133.M. Mascini and D. Moscone, *Anal. Chim. Acta*, 1986, **179**, 439.
134.J. Z. Stemple, K. M. Rusin and T. L. Fare, *Anal. Chem.*, 1991, **63**, 1050.
135.Y. Ikarashi, T. Sasahara and Y. Maruyama, *J. Chromatogr.*, 1985, **322**, 191.
136.M. G. Garguilo, N. Huynh, A. Proctor and A. C. Michael, *Anal. Chem.*, 1993, **65**, 523.
137.M. Israel and B. Lesbats, *J. Neurochem*., 1982, **39**, 248.
138.N. Korbakov, P. Timmerman, N. Lidich, B. Urbach, A. Sa'ar and S. Yitzchaik, *Langmuir*, 2008, **24**, 2580.
139.A. Zacharias and D. A. Dougherty, *Trends Pharm. Sci.*, 2002, **23**, 281.
140.C. A. Ma and D. A. Dougherty, *Chem. Rev.*, 1997, **97**, 1303.
141.Z. Chen, X. Ren, X. Meng, D. Chen, C. Yan, J. Ren, Y. Yuan and F. Tang, *Biosens. Bioelectron*., 2011, **28**, 50.
142.H. Benveniste, J. Drejer, A. Schousboe and N. H. Diemer, *J. Neurochem*, 1984, **43**, 1369.
143.A. I. Faden and R. P. Simon, *Ann. Neurol*., 1988, **3**, 623.
144.J. D. Rothstein, L. J. Martin and R. W. Kunci, *N. Engl. J. Med.*, 1992, **326**, 1464.
145.D. Liu, *Mol. Chem. Neuropathol.*, 1994, **23**, 77.
146.S. L. Leib, Y. S. Kim, D. M. Ferriero and M. G. Tuber, *J. Infect. Dis.*, 1996, **173**, 166.
147.M. Bhuyan, E. Katayev, S. Stadlbauer, H. Nonaka, A. Ojida, I. Hamachi and B. Koenig, *Eur. J. Org. Chem.*, 2011, **15**, 2807.
148.L. Wang, X. He, Y. Guo, J. Xu and S. Shao, *Beilstein J. Org. Chem.*, 2011, **7**, 218.
149.R. A. Doong, P.-S. Lee and K. Anitha, *Biosens. Bioelectron.*, 2010, **25**, 2464.
150.H. Guan, P. Zhou, X. Zhou and Z. He, *Talanta*, 2008, **77**, 319.
151.M. Chadlaoui, B. Abarca, R. Ballesteros, C. Ramirez de Arellano, J. Aguilar, R. Aucejo and E. Garcia-Espana, *J. Org. Chem.*, 2006, **71**, 9030.
152.S.-Y. Liu, L. Fang, Y.-B. He, W.-H. Chan, K.-T. Yeung, Y.-K. Cheng and R.-H. Yang, *Org. Lett.*, 2005, **7**, 5825.
153.J. P. Issberner, C. L. Schauer. B. A. Trimmer and D. R. Walt, *J. Neurosci. Methods*, 2002, **120**, 1.
154.M. Bonizzoni, L. Fabbrizzi, G. Piovani and A. Taglietti, *Tetrahedron*, 2004, **60**, 11159.
155.V. I. Skvortsova, K. S. Raevskii, A. V. Kovalenko, V. S. Kudrin, L. A. Malikova, M. A. Sokolov, A. A. Alekseev, E. I. Gusev, *Neuroscience and Behavioral Physiology* , 2000, **30**, 491.
156. J. Storm-Mathisen, N. C. Danbolt, F. Rothe, R. Trop, N. Zhang, J. E. Aas, B. I. Kanner, I. Langmoen, O. P. Ottersen, *Prog. Brain. Res.,* 1992, **94**, 225.
157.H. Aït-Haddou, S. L. Wiskur, V. M. Lynch and E. V. Anslyn, *J. Am. Chem. Soc.*, 2001, **123**, 11296.
158.G.-Y. Qing, Z.-H. Chen, F. Wang, X. Yang, L.-Z. Meng and Y.-B. He, *Chinese J. Chem.*, 2008, **26**, 721.
159.Y.-M. Li, Y. Qu, E. Vandenbussche, L. Arckens and F. Vandesande, *J. Neurosc. Meth.*, 2001, **105**, 211.
160.A. P. de Silva, H. Q. N. Gunaratne, C. McVeigh, G. E. M. Maguire, P. R. S. Maxwell and E. O'Hanlon, *Chem. Commun.*, 1996, **18**, 2191.
161.G. He, N. Yan, H. Cui, T. Liu, L. Ding and Y. Fang, *Macromolecules*, 2011, **44**, 7096.
162.C. V. Durgadas, C. P. Sharma and K. Sreenivasan, *Analyst*, 2011, **136**, 933.
163.Q. Zeng, C. K. W. Jim, J. W. Y. Lam, Y. Dong, Z. Li, J. Qin and B. Z. Tang, *Macromol. Rapid Commun.*, 2009, **30**, 170.
164.E. K. Feuster and T. E. Glass, *J. Am. Chem. Soc.*, 2003, **125**, 16174.
165.R. J. Wurtman, F. Hefti and E. Melamed, *Pharmacol. Rev.*, 1981, **32**, 315.
166.C.-T. Chen and Y.-C. Chen, *Chem. Commun.*, 2010, **46**, 5674.
167.R. Freeman, T. Finder, L. Bahshi and I. Willner, *Nano Lett.*, 2009, **9**, 2073.
168.D. M. Bailey, A. Hennig, V. D. Uzunova and W. M. Nau, *Chem. Eur. J.*, 2008, **14**, 6069.
169.S. Atilgan and E. U. Akkaya, *Tetrahedron Lett.*, 2004, **45**, 9269.
170.B. T. Nguyen and E. V. Anslyn, *Coord. Chem. Rev.*, 2006, **250**, 3118.
171.L. Zhu and E. V. Anslyn, *J. Am. Chem. Soc.*, 2004, **126**, 3676.
172.T. Zhang and E. V. Anslyn, *Org. Lett.*, 2007, **9**, 1627.
173.A. Hennig, H. Bakirci and W. M. Nau, *Nat. Methods*, 2007, **4**, 629.
174.J. Ruta, S. Perrier, C. Ravelet, J. Fize and E. Peyrin, *Anal. Chem.*, 2009, **81**, 7468.
175.T. Hasegawa, M. Hagihara, M. Fukuda, S. Nakano, N. Fujieda and T. Morii, *J. Am. Chem. Soc.*, 2008, **130**, 8804.
176.J.-H. Park, E. O. Ganbold, D. Uuriintuya, K. Lee and S.-W. Joo, *Chem. Commun.*, 2009, **47**, 7354.
177.A. M. Patel, A. Dutta and H. Huang, *Anal. Bioanal. Chem.*, 2011, **400**, 3035.
178.S.-J. Chena, C.-C. Huang and H.-T. Chang, *Talanta*, 2010, **81**, 493.
179.Y. Yoneyama, S. Suzuki, R. Sawa, Y. Otsubo, G. G. Power, T. Araki, *Am. J. obstet. Gynecol.,* 2000, **182**, 1200.
180.B. P. Ramakers, P. Pickkers, A. Deussen, G. A. Rongen, P. van der Broek, J. G. van der Hoeven, P. Smits, N. P. Riksen, Curr. *Drug Metab.* 2008, 9, 679.
181.T. V. Dunwiddie and S. A. Masino, *Annu. Rev. Neurosci.*, 2001, **24**, 31.
182.K. A. Jacobsen and Z.-G. Gao, *Nat. Rev. Drug. Discov.*, 2006, **5**, 247.

183.H. E. Gruber, M. E. Hoffer, D. R. McAllister, P. K. Laikind, T. A. Lane, G. W. Schmid-Schoenbein and R. L. Engler, *Circulation*, 1989, **80**, 1400.
184.L. A. Conlay, J. A. Conant, F. deBros and R. Wurtman, *Nature*, 1997, **389**, 136.
185.M. Castro-Gago, F. Camina, S. Lojo, S. Rodriguez-Segade and A. Rodriguez-Nunez, *Eur. J. Clin. Chem. Clin. Biochem.*, 1992, **30**, 761.
186.L. Bekar, W. Libionka, G. F. Tian, Q. Xu, A. Torres, X. Wang, D. Lovatt, E. Williams, T. Takano, J. Schnermann, R. Bakos and M. Nedergaard, *Nat. Med.*, 2008, **14**, 75.
187.A. D. Ellington and J. W. Szostak, *Nature*, 1990, **346**, 818.
188.R. Green, A. D. Ellington, D. P. Bartel and J. W. Szostak, *Methods*, 1991, **2**, 75.
189.M. Famulok and J. W. Szostak, *Angew. Chem. Int. Ed.*, 1992, **31**, 979.
190.W. Xu and Y. Lu, *Anal. Chem.*, 2010, **82**, 574.
191.J. Liu and Y. Lu, *Angew. Chem. Int. Ed.*, 2006, **45**, 90.
192.N. Lu, C. Shao and Z. Deng, *Chem. Commun.*, 2008, **46**, 6161.
193.Y. Xiang, Z. Wang, H. Xing, N. Y. Wong and Y. Lu, *Anal. Chem.*, 2010, **82**, 4122.
194.D. E. Huizenga and J. W. Szostak, *Biochemistry*, 1995, **34**, 656.
195.D. Y. Wang, B. H. Lai and D. Sen, *J. Mol. Biol.*, 2002, **318**, 33.
196.J. Liu, J. H. Lee and Y. Lu, *Anal. Chem.*, 2007, **79**, 4120.
197.H. Urata, K. Nomura, S.-I. Wada and M. Akagi, *Biochem. Biophys. Res. Commun.*, 2007, **360**, 459.
198.F. Li, J. Zhang, X. Cao, L. Wang, D. Li, S. Song, B. Ye and C. Fan, *Analyst*, 2009, **134**, 1355.
199.Y. Xiang, A. Tong and Y. Lu, *J. Am. Chem. Soc.*, 2009, **131**, 15352.
200.Y. Xiang, Z. Wang, H. Xing, N. Y. Wong and Y. Lu, *Anal. Chem.*, 2010, **82**, 4122.
201.J. Liu and Y. Lu, *Angew. Chem. Int. Ed.*, 2006, **45**, 90.
202.J. Liu and Y. Lu, *Nat. Protoc.*, 2006, **1**, 246.
203.J. Liu and Y. Lu, *Anal. Chem.*, 2003, **75**, 6666.
204.N. L. Rosi and C. A. Mirkin, *Chem. Rev*., 2005, **105**, 1547.
205.H. Liu, Y. Li, S. Wang, Y. Li, N. Wang, J. Xiao, X. Xu and D. Zhu, *Adv. Mater*., 2005, **17**, 2811.
206.F. He, Y. Tang, S. Wang, Y. Li and D. Zhu, *J. Am. Chem. Soc.*, 2005, **127**, 12343.
207.X. Liu, Z. Zhou, L. Zhang, Z. Tan, G. Shen and R. Yu, *Chin. J. Chem.*, 2009, **27**, 1855.
208.W. A. Zhao, C. William, C. F. L. Jeffrey, A. B. Michael and Y. F. Li, *Chem. Commun.*, 2007, **36**, 3729.
209.E. L. Null and Y. Lu, *Analyst*, 2010, **135**, 419.
210.X.-B. Zhang, Z. Wang, H. Xing, Y. Xiang and Y. Lu, *Anal. Chem.*, 2010, **82**, 5005.
211.S. Nishizawa, Y. Sato, Z. Xu, K. Morita, M. Li and N. Teramae, *Supramol. Chem.*, 2010, **22**, 467.
212.B. Honig and R. Rohs, *Nature*, 2011, **470**, 472.
213.Z. Xu, Y. Sato, S. Nishizawa and N. Teramae, *Biosens. Bioelectron.*, 2011, **26**, 4733.
214.Y. S. Kim and J. Jurng, *Analyst*, 2011, **136**, 3720.
215.A. Kidd, V. Guieu, S. Perrier, C. Ravelet and E. Peyrin, *Anal. Bioanal. Chem.*, 2011, **401**, 3229.
216.S. Redon, S. Bombard, M. A. Elizondo-Riojas and J. C. Chottard, *Nucleic Acids Res.*, 2003, **31**, 1605.
217.V. Guieua, C. Raveleta, S. Perriera, Z. Zhua, S. Cayezb and E. Peyrina, *Anal. Chim. Acta*, 2011, **706**, 349.
218.P. Song, Y. Xiang, H. Xing, Z. Zhou, A. Tong and Y. Lu, *Anal. Chem.*, 2012, **84**, 2916.

Biographies

Dr. Tuhin Pradhan earned his Ph. D. in Physical Chemistry in 2009 under the direction of Profs. Ranjit Biswas and Jaydeb Chakrabarti at S. N. Bose National Centre for Basic Sciences (Jadavpur University), India. He continued his postdoctoral research in the same research institute for nearly one and a half years. He joined the laboratory of Prof. Jong Seung Kim at Korea University in Korea, as a Research Professor in 2010 and worked for three years. He is currently an Assistant Professor of Chemistry at Vel Tech Dr. RR & Dr. SR Technical University, India. He has co-authored 28 scientific publications in reputed international journals. His research includes studying medium dynamics and charge transfer reactions in complex media with the help of advanced spectroscopic techniques, electrochemistry, computational supramolecular chemistry, developing sensor materials for clinically important analytes.

Hyo Sung Jung was born in Seoul, Korea in 1983. He received his BS degree in chemistry from the Dankook University in 2006. He then joined Prof. Jong Seung Kim's lab and is involved in the design and synthesis of fluorogenic probes for detecting specific metal ions or biospecies. He received his Ph.D. in organic chemistry from the Korea University in 2013. He has co-authored 25 scientific publications and 6 patents so far. His current research interests include the design and synthesis of fluorogenic probes for biospecies and their applications to the field of DDS.

Joo Hee Jang was born in Seoul, Korea in 1988. She received a B. S. (2007) from Chungju National University, Korea. She then joined Prof. Jong Seung Kim's lab as a Masters/Doctoral student. Her main research interests concern 'Design and synthesis of fluorescent reporter and its bio applications.'

Tae Woo Kim received his Ph. D. in organic chemistry from the Seoul National University in 2001 under the guidance of Prof. Jong-In Hong on host-guest chemistry. From 2002 to 2006, he held a postdoctoral fellowship with Prof. Eric T. Kool at the Stanford University in USA, where he investigated the mechanisms underlying the fidelity of DNA polymerase. In 2007, he returned to Korea and joined the POSTECH Biotech Center. Since 2009, he has been Assistant Professor in the Graduate School of East-West Medical Science at the Kyung Hee University. His current interests include the design, development, and study of organelle-selective sensors and bioconjugation.

Chulhun Kang received his Ph. D. in Biochemistry from the Department of Biochemistry and Biophysics at Iowa State University. Since 1997, he has served as a faculty member at Kyung Hee University and is currently a Professor of the Department of Medical Science. To date, he has co-authored about 50 scientific publications and 10 domestic and international patents in the fields of organic chemistry and biological science.

Jong Seung Kim received a Ph. D. from Department of Chemistry and Biochemistry at Texas Tech University. He then worked in Department of Chemistry at University of Houston as a research fellow. Currently he is a professor in Department of Chemistry at Korea University at Seoul, Korea. To date, he published more than 300 scientific publications and 50 domestic and international patents.

<Table of Contents>

This review focuses on the chemosensors for neurotransmitter published for the last 12 years, covering biogenic amines (dopamine, epinephrine, norepinephrine, serotonin, histamine and acetylcholine), amino acids (glutamate, aspartate, GABA, glycine and tyrosine), and adenosine.